SPERRY
SUPPORT SERVICES

[redacted]

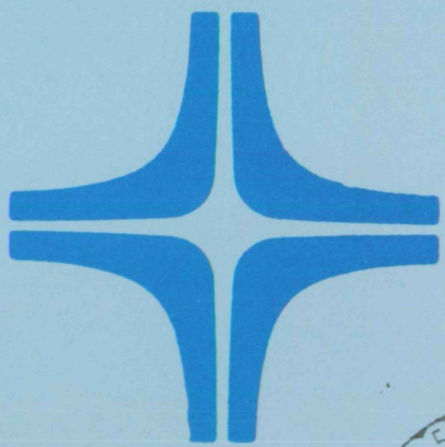

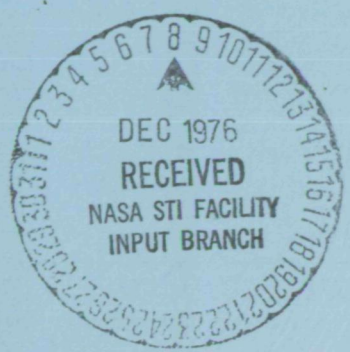

Sperry is a Division of Sperry Rand Corporation

October 29, 1976

ANALYSES OF ACPL THERMAL/FLUID CONDITIONING SYSTEM

Prepared by: L A Stephen
L. A. Stephen
Senior Staff Engineer

L H Usher
L. H. Usher
Principal Investigator

Prepared for

National Aeronautics and Space Administration
George C. Marshall Space Flight Center
Marshall Space Flight Center, Alabama
Under Contract NAS8-32016 Mod. 2

By

Sperry Support Services
716 Arcadia Circle
Huntsville, Alabama 35801

TABLE OF CONTENTS

1.0 SUMMARY

Results of engineering analyses performed under Contract NAS8-32016, Modification 2 are reported herein. Initial computations were made using a modified control transfer function where the systems performance was characterized parametrically using a previously developed analytical model. The analytical model was then revised to represent the latest expansion chamber fluid manifold design and further systems performance predictions were made. Parameters which were independently varied in these conputations are listed below:

- Controller transfer function constants including the integrator gain and the proportional gain.
- Heat transfer coefficient between the fluid and expansion chamber wall.
- Fluid flow rate.

Systems predictions which were used to characterize performance are primarily transient computer plots comparing the deviation between average chamber temperature and the chamber temperature requirement. Additional computer plots were prepared to depict the following characteristics:

- Control function transient behavior.
- Fluid flow rates from hot, cold and bypass sources as a function of time.
- Transient pipe surface temperatures for nodal representations as a function of time.
- Transient fluid temperature for all nodal representations as a function of time.

Results of parametric computations with the latest fluid manifold design, indicate that systems performance requirements were most closely approached by selection of the following combination of parameters:

- Integrator gain constant, $8 \leq K_L \leq 11$
- Proportional gain constant, $2 \leq \tau K_L \leq 5$
- Fluid flow rate, $\dot{\omega}$ = 6.6 gpm.

Presented in Table I is a summary of each computer case identification and the calculated chamber temperature deviations from the required value. Initial parametric studies of the control transfer function revealed favorable behavior in limiting temperature deviations and damping the temperature oscillations. Computations using the updated analytical model, in computer Cases 33 through 35, indicate that the maximum temperature deviation predictions closely approach the specification of $\pm$0.1°C.

2.0 INTRODUCTION

2.1 Background - Sperry Support Services performed engineering analyses of the Atmospheric Cloud Physics expansion chamber fluid thermal conditioning system under Contract NAS8-32016. The purpose of this original analysis, as reported in Reference 1, was to evaluate and determine systems components and a design configuration which would lead to a feasible design approach. The hardware and the baseline control system available for evaluation were specified by MSFC as design constraints.

Subsequent to completion of the required engineering analyses, MSFC made improvements in the expansion chamber internal fluid flow channels, fluid piping manifold designs and in the fluid thermal controller transfer function. It was necessary to incorporate these changes into the existing analytical model and to perform parametric investigations to determine systems performance characteristics. Results of analyses are to be used to support hardware design development activities at MSFC.

2.2 Analytical Techniques - The analytical techniques employed in these analyses are the same as those of Reference 1. The analytical model as originally developed is depicted schematically in Figure 1.

Initial computations performed under this contract modification consisted of changes to the control transfer function used in conjunction with the original analytical model. The equation used to simulate the controller function in terms of voltage is,

$$e_o = K_L \tau e_{in} + K_L \int_0^t e_{in}\, dt$$

where,

e_o = Controller output voltage
e_{in} = Input voltage to controller
K_L = Integrator gain constant
$K_L\tau$ = Proportional gain constant
t = Time

The input voltage to the controller is defined as,

$$e_{in} = 0.4\ (T_R - T_C)$$

where,

T_R = Required temperature, °C
T_C = Chamber temperature, °C (Average of nodes 1051, 1052, 1053)

Controller output voltage, e_o, was formulated to selectively actuate servovalves based on the following logic.

- ($e_o \leq$ - 7 volts) corresponds to 100 percent opening of the valve associated with the cold reservoir. Under this condition the other two valves would be closed.
- ($e_o \geq$ + 7 volts) corresponds to 100 percent opening of the valve associated with the hot reservoir. Under this condition the other two valves would be closed.
- ($0 > e_o > -7$ volts) the valve supplying cold fluid is open a proportionate interval of time to the ratio of $|e_o/7|$. The remaining time interval $(1 - |\frac{e_o}{7}|$ is allocated to open the by-pass fluid valve. The other valve is closed.
- ($0 < e_o < +7$ volts) the valve supplying hot fluid is open a proportionate interval of time to the ratio of $|e_o/7|$. The remaining time interval $(1 - |\frac{e_o}{7}|)$ is allocated to open the by-pass fluid valve. The other valve is closed.

- ($\ddot{e}_o = 0$) the by-pass valve is open and other valves closed.

The above control equations and logic were programmed into the SINDA program input data. These programmed functions act as boundaries on the analytical model. After completion of initial investigations, the analytical model was modified to represent the fluid manifold design. A sketch of the modified analytical model is shown in Figure 2. A summary of materials and conditions which were represented in this model are tabulated as follows:

- Supply lines and manifold material - Tygon tubing 0.16 cm thick.
- Working fluid - Coolanol 20.
- Thermal insulation - 1.27 cm thickness of polyurethane. External surfaces of insulation were allowed to transfer heat by convection to a 20°C boundary.
- Convective heat transfer coefficients between the working fluid and the expansion chamber surfaces were calculated and utilized in parametric investigations as follows:

(a) $\bar{h}c = 0.023 \frac{k}{D_H} (Re_D)^{.8} P_r^{.33}$

where, $\bar{h}c$ is the average heat transfer coefficient k is liquid thermal conductivity

D_H is the channel hydraulic diameter
Re_D is the Reyonlds number
P_r is the Prandtl number.

(b) An equation was developed to calculate thermal conductance between the liquid and the expansion chamber surfaces based upon heat transfer information received from MSFC. The equation used follows,

$$\bar{h}cA = .01617 [\dot{\omega}]^{.33} \text{ BTU/sec°F}$$

where,

$\bar{h}c$ is the average heat transfer coefficient
A is the surface area
$\dot{\omega}$ is the fluid flow rate, lb_m/hr.

The value of $\bar{h}cA$ was proportioned according to the length of the pipes simulating the chamber for Cases 30 and 32. After the model was modified to reflect the new manifold and crossflow the $\bar{h}cA$ value was proportioned according to the number of flow channels. Values used to calculate conductions between the working fluid and expansion chamber surfaces are listed below for Cases 33 through 35:

- Each TOP disc = $\bar{h}cA * \frac{15}{160}$ (see Figure 2)
- Each cylindrical section = $\bar{h}cA * \frac{50}{160}$ (see Figure 2)
- Each bottom disc = $\bar{h}cA * \frac{15}{160}$ (see Figure 2).
- The thermal system was initialized as follows,
  (a) Cold reservoir, -45.6°C
  (b) Hot reservoir, 54.4°C
  (c) Volume cold reservoir, 106 liters
  (d) Volume hot reservoir, 53 liters.

Parametric studies were made with each analytical model using the UNIVAC 1108 ELT processor.

3.0 RESULTS OF ANALYSES

Selected computer plots containing the transient behavior of the control function, fluid flow rates from respective reservoirs and predicted expansion chamber temperature deviation from required values are contained in this report. Additional plotted data were generated which illustrate detailed liquid and piping system transients. The detailed plots were included in a separate addendum to this report.

3.1 Results for Control Function Update - The existing analytical model of the thermal system (Figure 1) was utilized with control function parameter variations to obtain preliminary predictions on systems thermal

behavior. Parametric studies made correspond to computer Cases designated as 30a through 30e, 31a through 31e, and 32a through 32f. Convective heat transfer coefficients in computer Case 31 were calculated by equation (a) as referred to in the Analytical Techniques Section. Heat transfer coefficients obtained from MSFC were used in Computer Cases 30 and 32. Results of analyses as depicted graphically in Figures 3 through 18 indicate that, for the fluid flow rate investigated (8.3 liters/minute), heat transfer rates by equation (a) would be insufficient to maintain the required expansion chamber temperature transients. When the higher convection heat transfer coefficients of equation (b) were applied in Cases 30 and 32, results of analyses indicated better heat transfer rates since the predicted temperature deviations from required values in Cases 30 and 32 were less than those of Case 31 (see Table I). Although the deviations calculated in Cases 30 and 32 were significantly less than those of Case 31, they were still too large to meet the required chamber temperature deviation of $\pm$.1°C. At this time the model was modified to reflect the new manifold and to simulate the crossflow fluid system.

3.2 Results for Fluid Network and Control Function Updates - The calculated deviations are depicted graphically in Figures 19 through 31. A summary of significant technical considerations which have been determined in these analyses is presented graphically in Figures 32 and 33. These points are enumerated below:

- Figure 32 indicates that as the flowrate increases the temperature deviation decreases.
- Figure 33 indicates that as the proportionality gain constant (τK_L) approaches zero the temperature deviation becomes large. An optimum value of τK_L was estimated to exist between the values of 2 and 5.

Results of analyses with the latest manifold design generally show improved thermal control of the expansion chamber.

4.0 CONCLUSIONS AND RECOMMENDATIONS

The following trends and conclusions are based upon the computed systems performance characteristics:

- Fluid flow rates of 8.3 liters/minute or greater would be acceptable.
- Computations with up to 24.9 liters/minute flow rate generally showed that increased flow rates improved controllability.
- Parametric studies of the proportional gain constant indicate that optimum values of $K_L\tau$ should exist in the range of 2 to 5.
- Localized temperature excursions were predicted to occur during operational periods where the required expansion chamber temperature profile slope changes.
- Expansion chamber temperature control was improved by use of the latest fluid manifold design.
- Nodal representations of the expansion chamber top and bottom discs and the cylinder were utilized as arithmetic average temperatures in control equations. Also, expansion chamber temperature deviations from the requirement were based upon the arithmetic average expansion chamber temperatures as compared with required values. In the detailed computer plots of the Appendix to this report, it is evident that temperature differentials were predicted between the expansion chamber cylindrical section and the end discs. These differentials may be observed by examining the fifth plot of each case for configuration 5. For example, the first plot depicting these differentials may be found on page 196 for Case 33a. It is concluded that the fluid flow through the discs and the cylinder should be properly proportioned to minimize temperature gradients in the chamber.

It is recommended that additional analyses be performed to accomplish the following scope of work:

- Develop a detailed analytical model to represent the expansion chamber surfaces.
- Integrate the detailed thermal representation of the chamber with the current analytical model as detailed herein.
- Predict operational characteristics of the detailed expansion chamber model to determine and select locations for control sensors. Also, to determine necessary fluid flow rates to be admitted to the cylindrical and end discs to minimize temperature gradients in the expansion chamber.

- Verify the analytical model by use of MSFC supplied experimental data.
- Computations should be performed using the verified analytical model to predict the range of experiment operational constraints. These constraints would include variations of ambient temperature, various required expansion chamber temperature profiles, fluid flow rates, and optimization of fluid reservoir sizes.
- The verified analytical model would be coupled and modeled to interface the experiment with the chilling and heating units associated with the Spacelab vehicle. This would be termed a total thermal systems model.
- Final computations would be performed to predict performance characteristics for planned mission using the total thermal systems model.

REFERENCES

1. Schultz, W. E., Stephen, L. A., and Usher, L. H., "Final Report Atmospheric Cloud Physics Laboratory Project Study," Sperry Support Services, June 22, 1976.

TABLE I. SUMMARY OF CASES

CASE NO.	HEAT TRANSFER COEFFICIENTS USED	LOCAL TEMPERATURE SPIKE DEVIATION MINIMUM °C	LOCAL TEMPERATURE SPIKE DEVIATION MINIMUM °C	TEMPERATURE DEVIATION EXCLUDING SPIKES MINIMUM °C	TEMPERATURE DEVIATION EXCLUDING SPIKES MAXIMUM °C	τ	K_L	FLOWRATE GPM	CROSSFLOW USED IN MODEL	OUTPUT VOLTAGE RANGE MINIMUM VOLTS	OUTPUT VOLTAGE RANGE MAXIMUM VOLTS	PROPORTIONATE FLOW TIME FOR EACH MODE (DIMENSIONLES) HOT MIN/MAX	COLD MIN/MAX	BYPASS MIN/MAX
30a	MSFC	-.81	.96	-.53	.47	11.	.2	2.2	NO	*	*	*	*	*
30b	MSFC	-2.8	2.55	-2.8	2.55	11.	.4	2.2	NO	*	*	*	*	*
30c	MSFC	-6.9	6.9	-6.9	6.9	11.	.8	2.2	NO	*	*	*	*	*
30d	MSFC	-5.7	5.7	-5.7	5.7	8.	.4	2.2	NO	*	*	*	*	*
30e	MSFC	-3.5	3.8	-3.5	3.8	14.	.4	2.2	NO	*	*	*	*	*
31a	SPERRY	-12.8**	-4.3**	-2.7	2.1	11.	.2	2.2	NO	*	*	*	*	*
31b	SPERRY	-11.4**	-3.3**	-1.8	1.5	11.	.4	2.2	NO	*	*	*	*	*
31c	SPERRY	-12.9**	-4.4**	-1.3	1.3	11.	.8	2.2	NO	*	*	*	*	*
31d	SPERRY	-11.7**	-3.6**	-2.4	1.6	8.	.4	2.2	NO	*	*	*	*	*
31e	SPERRY	-12.9**	-4.4**	-1.4	1.3	14.	.4	2.2	NO	*	*	*	*	*
32a	MSFC	-.80	.96	-.52	.44	11.	.2	2.2	NO	-2.4	-1.	0./0.	.12/.38	.62/.88
32b	MSFC	-1.2	.96	-.53	.52	11.	.1	2.2	NO	-2.5	-1.	0./0.	.16/.34	.66/.84
32c	MSFC	-1.77	1.07	-.83	.79	11.	.05	2.2	NO	-2.0	-1.	0./0.	.16/.32	.68/.84
32d	MSFC	-2.6	1.56	-2.6	1.56	11.	.025	2.2	NO	-2.0	-2.0	0./0.	.16/.32	.68/.84
32e	MSFC	-1.3	.91	-.79	.91	8.	.1	2.2	NO	-2.5	-1.	0./0.	.16/.34	.66/.84
32f	MSFC	-1.2	.98	-.40	.40	14.	.1	2.2	NO	-2.5	-1.	0./0.	.16/.34	.66/.84
33a	MSFC	-.46	.57	-.20	.10	11.	.2	2.2	YES	-2.9	-.6	0./0.	.06/.40	.60/.94
33b	MSFC	-.76	.96	-.44	.13	11.	.1	2.2	YES	-2.9	.2	0./0.	.02/.42	.58/.98
33c	MSFC	-.46	.64	-.33	.15	11.	.4	2.2	YES	-2.9	-.3	0./0.	.08/.42	.58/.92
33d	MSFC	-.20	.20	-.17	.18	11.	.8	2.2	YES	***	***	0./0.	***	***
34a	MSFC	-.26	.32	-.10	.08	11.	.2	4.4	YES	-1.8	-.24	0./0.	.04/.26	.74/.98
34b	MSFC	-.38	.48	-.22	.10	11.	.1	4.4	YES	-1.76	-.24	0./0.	.04/.26	.74/.98
34c	MSFC	-.15	.30	-.08	.08	11.	.4	4.4	YES	-1.84	-.32	0./0.	.04/.26	.74/.98
34d	MSFC	-.12	.21	-.11	.11	11.	.8	4.4	YES	-1.92	-.08	0./0.	.02/.28	.72/.98
34e	MSFC	-.24	.34	-.10	.14	8.	.4	4.4	YES	-1.88	-.24	0./0.	.04/.26	.74/.98
35a	MSFC	-.185	.23	-.085	.08	11.	.2	6.6	YES	-1.44	-.3	0./0.	.04/.2	.8/.96
35b	MSFC	-.31	.43	-.18	.12	11.	.1	6.6	YES	-1.41	-.33	0./0.	.04/.2	.8/.96
35c	MSFC	-.15	.21	-.07	.07	11.	.4	6.6	YES	-1.47	-.21	0./01	.02/.2	.8/.98
35d	MSFC	-.14	.115	-.12	.11	11.	.8	6.6	YES	***	***	0./0.	***	***

* DATA NOT OUTPUT FOR THESE RUNS
** CHAMBER TEMPERATURE COULD NOT BE MAINTAINED DURING STEEPEST DESCENT ALONG THE REQUIRED CHAMBER TEMPERATURE CURVE.
*** NO PLOTS AVAILABLE

NOTE: Double nodes exist at each location, representing the hardware and the fluid.
Solid nodes are X or XX.
Liquid nodes are 10X or 1XX.

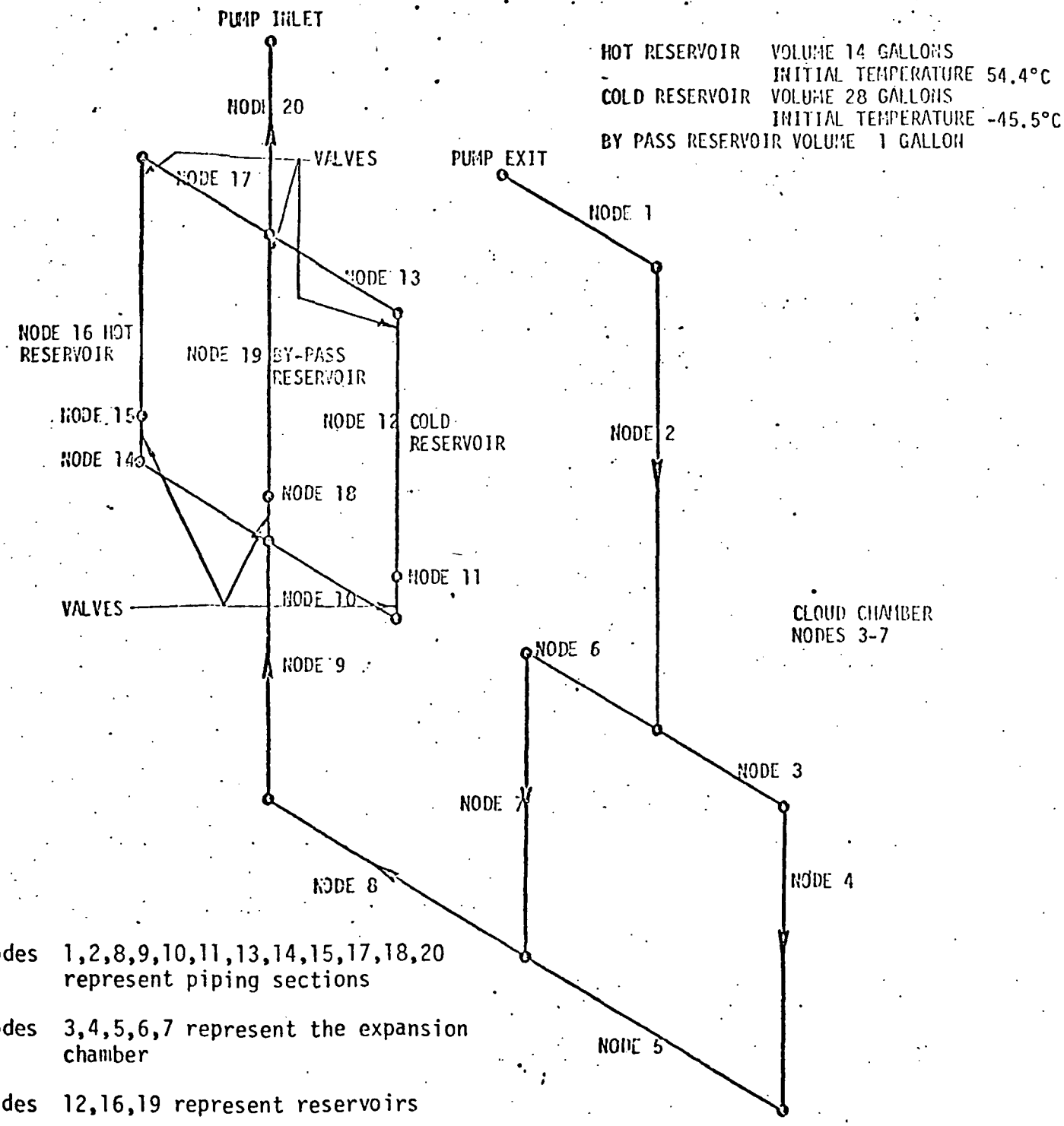

Nodes 1,2,8,9,10,11,13,14,15,17,18,20 represent piping sections

Nodes 3,4,5,6,7 represent the expansion chamber

Nodes 12,16,19 represent reservoirs

Figure 1. Analytical Model for Configuration "4".

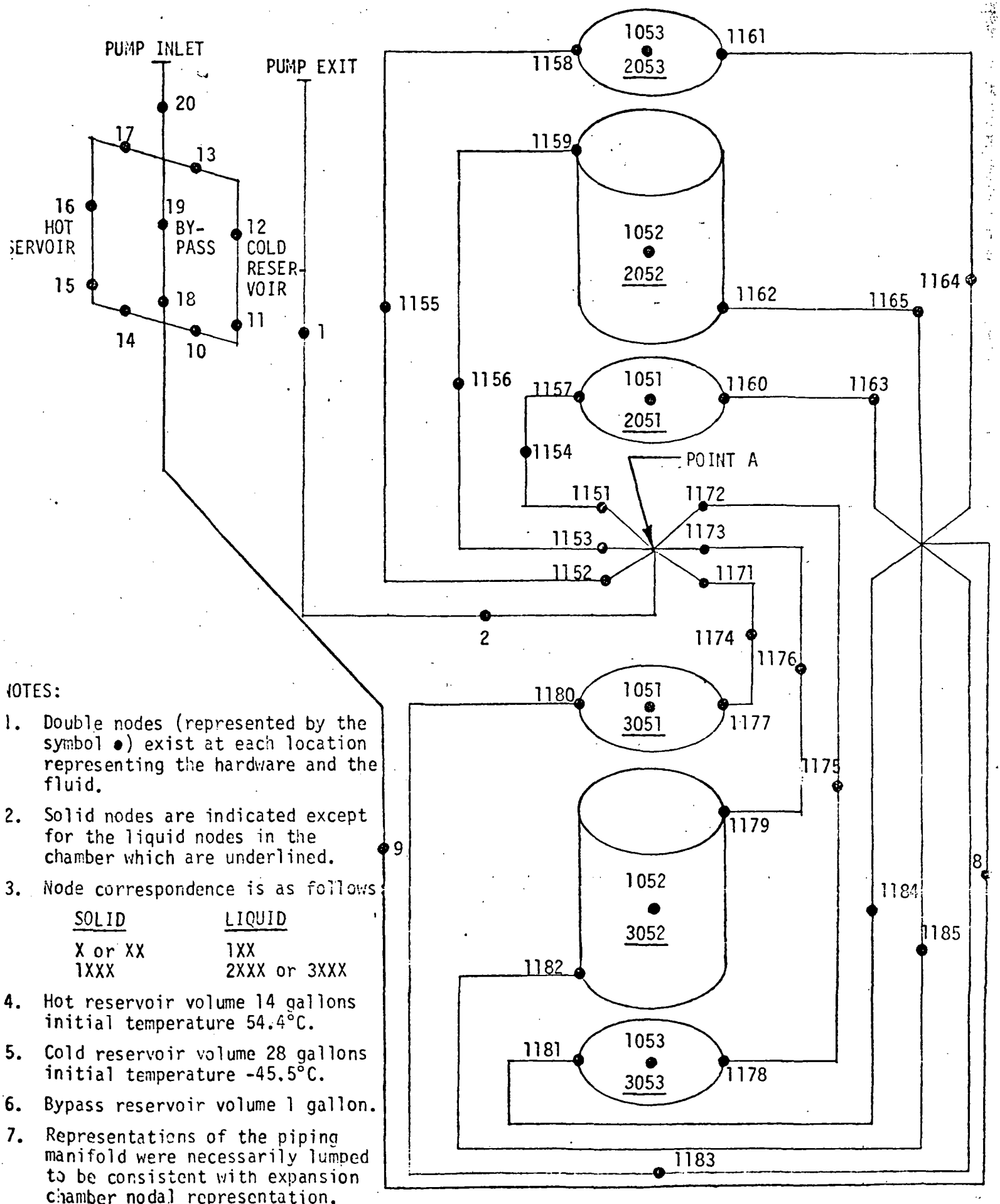

NOTES:

1. Double nodes (represented by the symbol •) exist at each location representing the hardware and the fluid.
2. Solid nodes are indicated except for the liquid nodes in the chamber which are underlined.
3. Node correspondence is as follows:

SOLID	LIQUID
X or XX	1XX
1XXX	2XXX or 3XXX

4. Hot reservoir volume 14 gallons initial temperature 54.4°C.
5. Cold reservoir volume 28 gallons initial temperature -45.5°C.
6. Bypass reservoir volume 1 gallon.
7. Representations of the piping manifold were necessarily lumped to be consistent with expansion chamber nodal representation.

Figure 2. Analytical Model for Configuration 5.

NOTES:

8. The lengths from the point labeled point "A" are the same as those supplied by MSFC; however, for model compatibility and modeling simplicity equivalent areas were substituted for the piping manifolds. The lengths and diameters of tubes modeled are listed below:

Length from Point A to node 1158, 1157, 1177, or 1178	= 53.34 cm.
Equivalent tube diameter used	= .64 cm.
Length from Point A to node 1159 or 1197	= 83.82 cm.
Equivalent tube diameter used	= 1.07 cm.
Length from Node 1158 to 1161, 1157 to 1160, 1180 to 1177, or 1181 to 1178	= 31.9 cm.
Equivalent tube diameter used	= 1.39 cm.
Length from Node 1159 to 1162, and 1179 to 1182	= 27.94 cm.
Equivalent tube diameter used	= 2.53 cm.

Figure 2. (Continued)

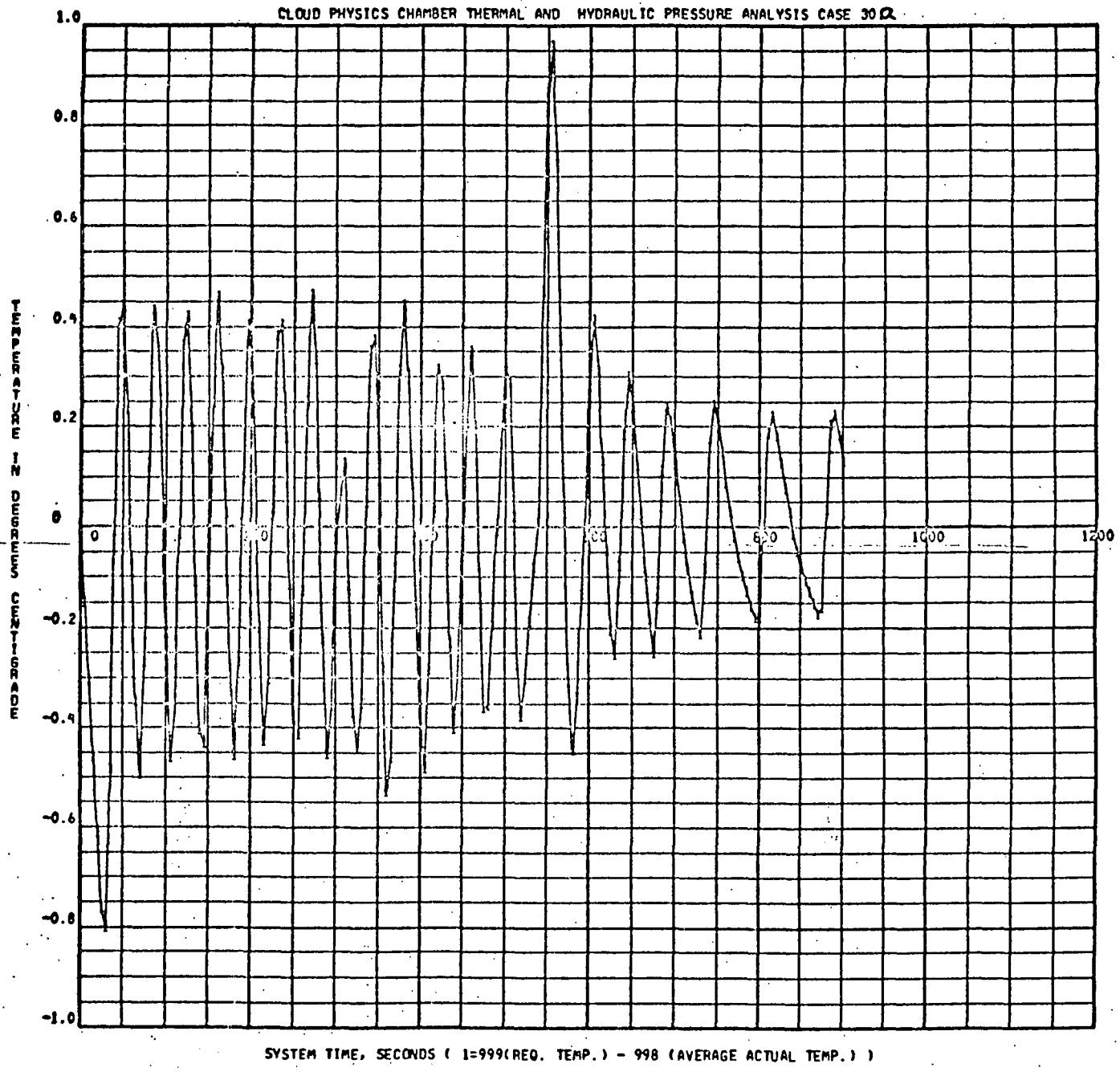

Figure 3. Configuration "4" Deviation from Required Temperature Case 30a.

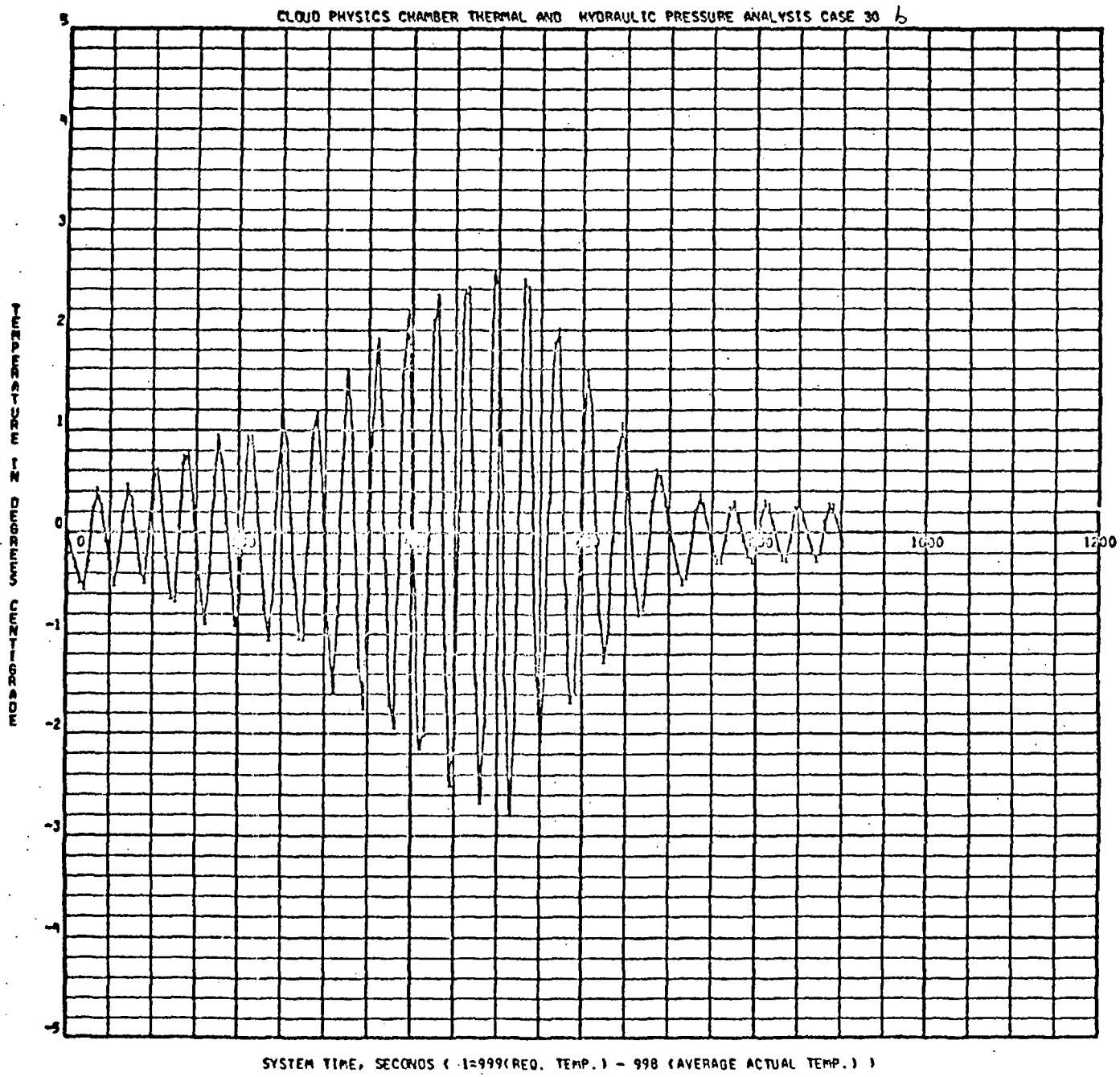

Figure 4. Configuration "4" Deviation from Required Temperature Case 30b.

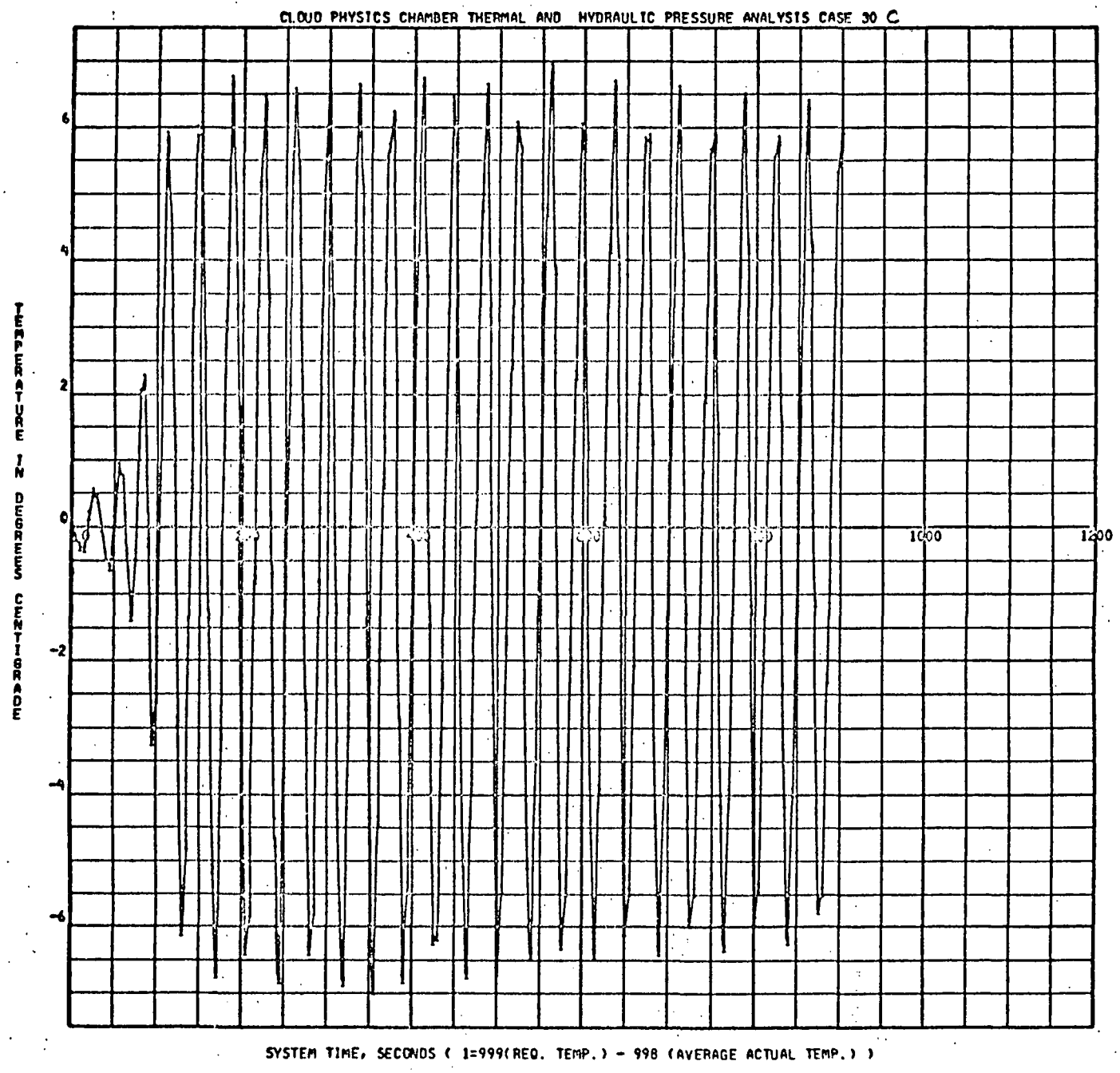

Figure 5. Configuration "4" Deviation from Required Temperature Case 30c.

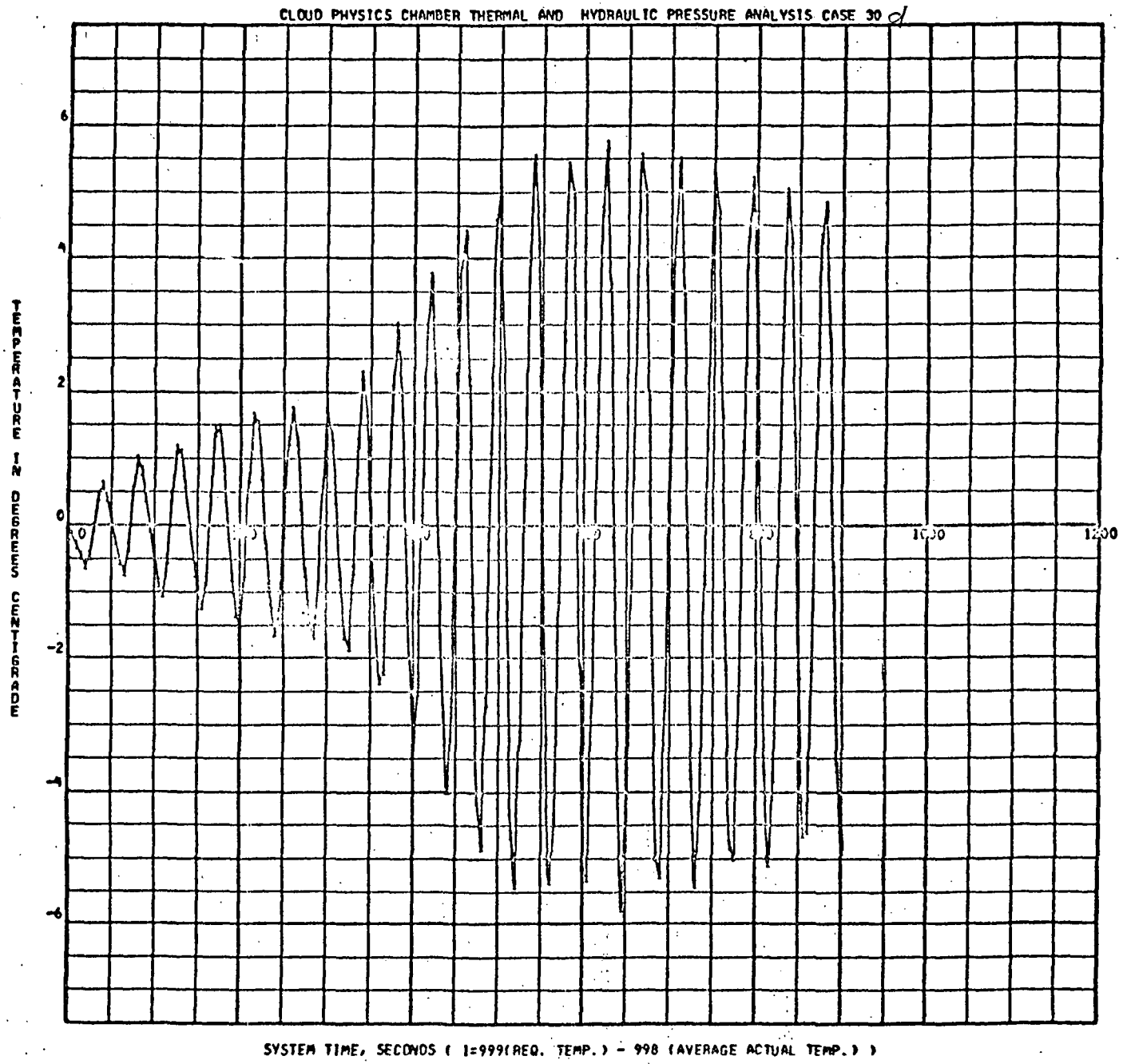

Figure 6. Configuration "4" Deviation from Required Temperature Case 30d.

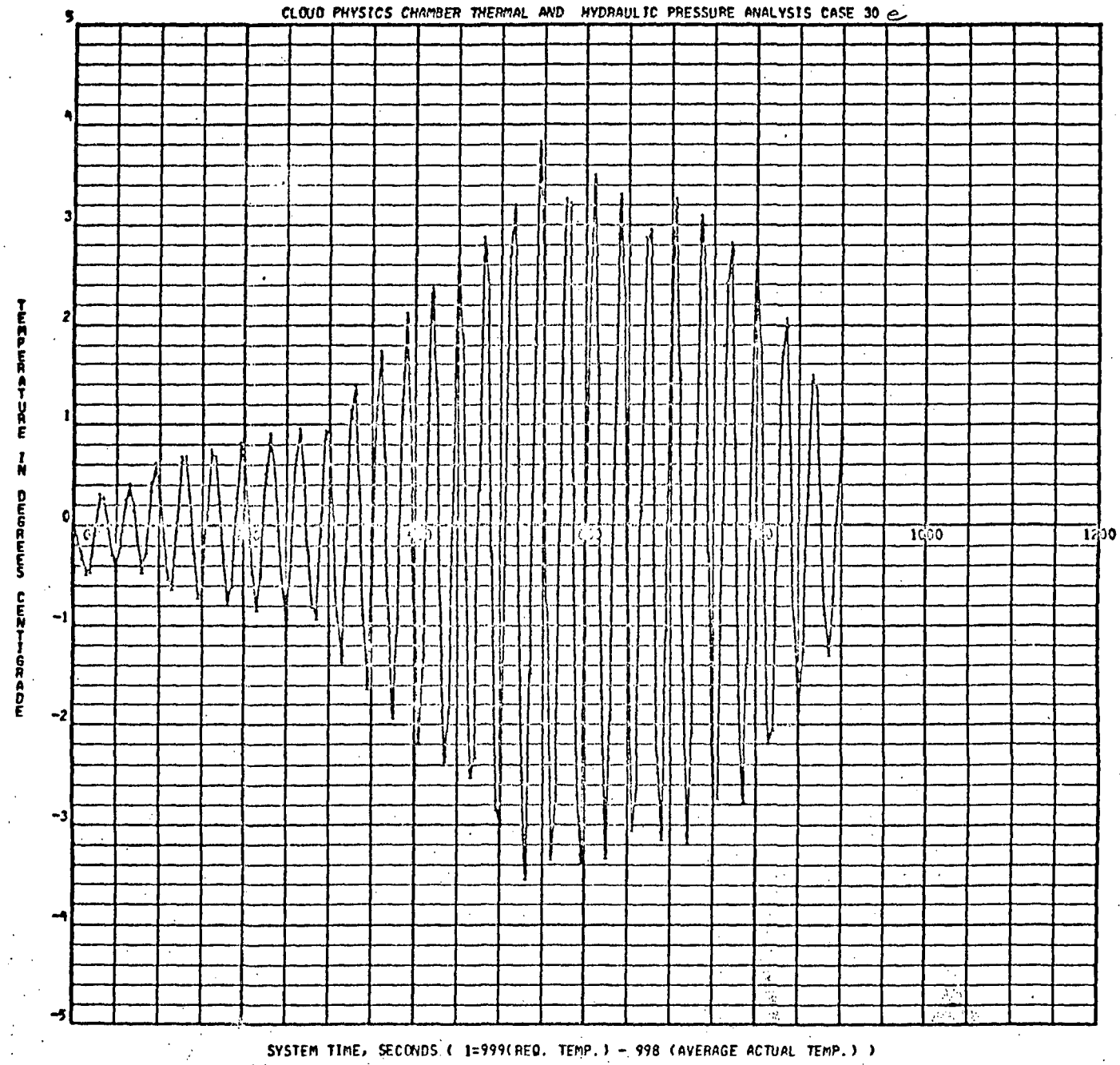

Figure 7. Configuration "4" Deviation from Required Temperature Case 30e.

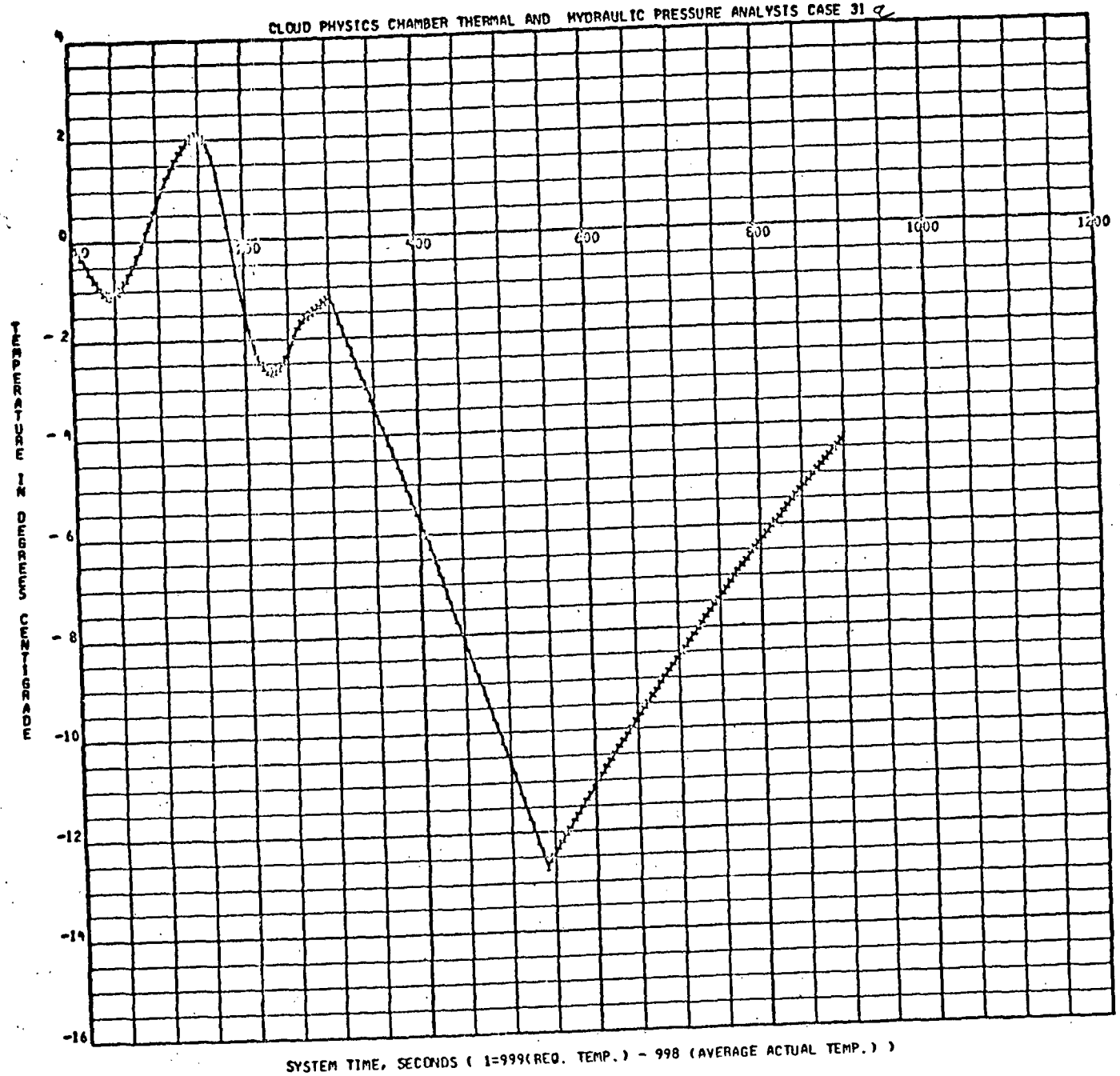

Figure 8. Configuration "4" Deviation from Required Temperature Case 31a.

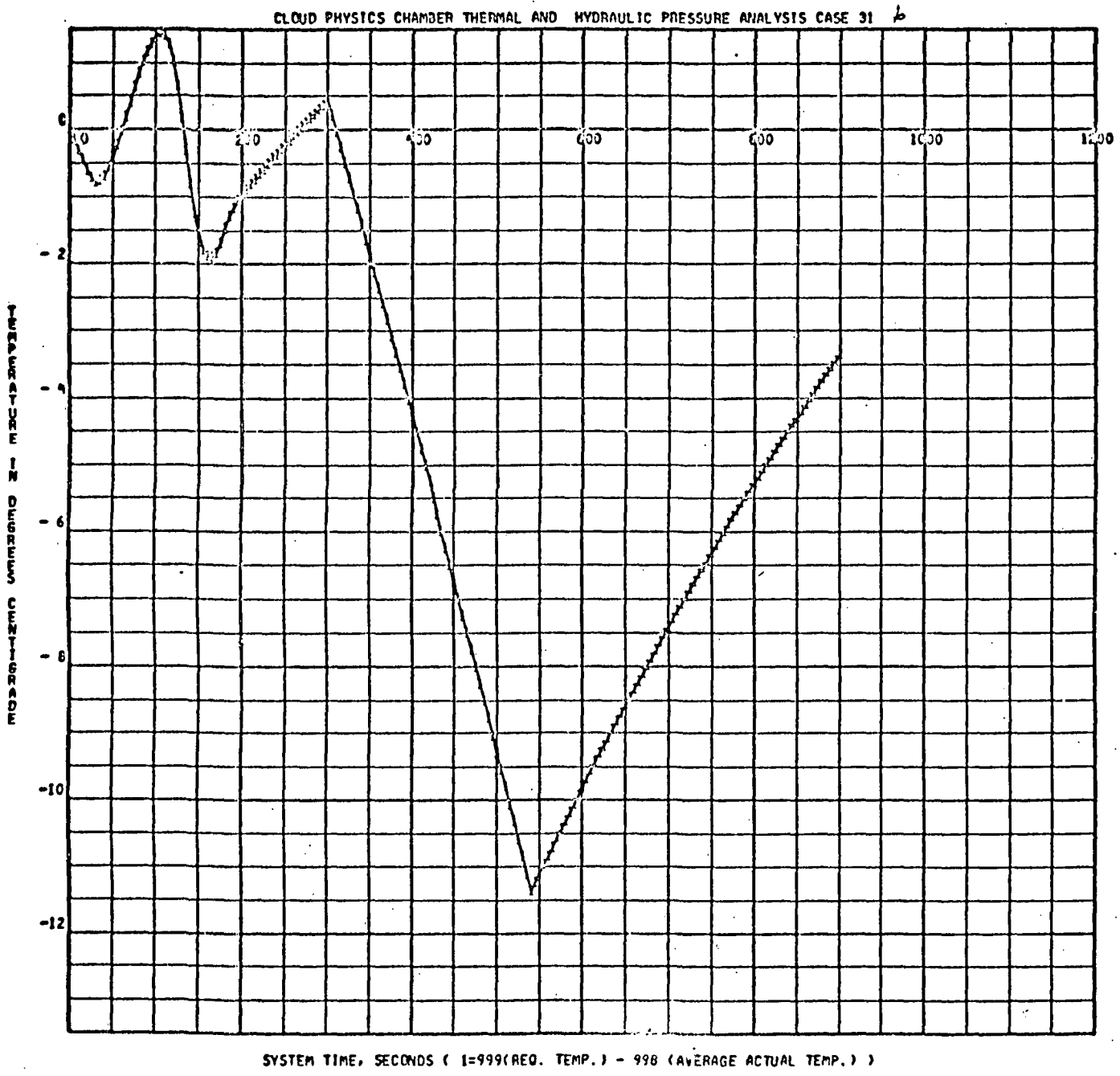

Figure 9. Configuration "4" Deviation from Required Temperature Case 31b.

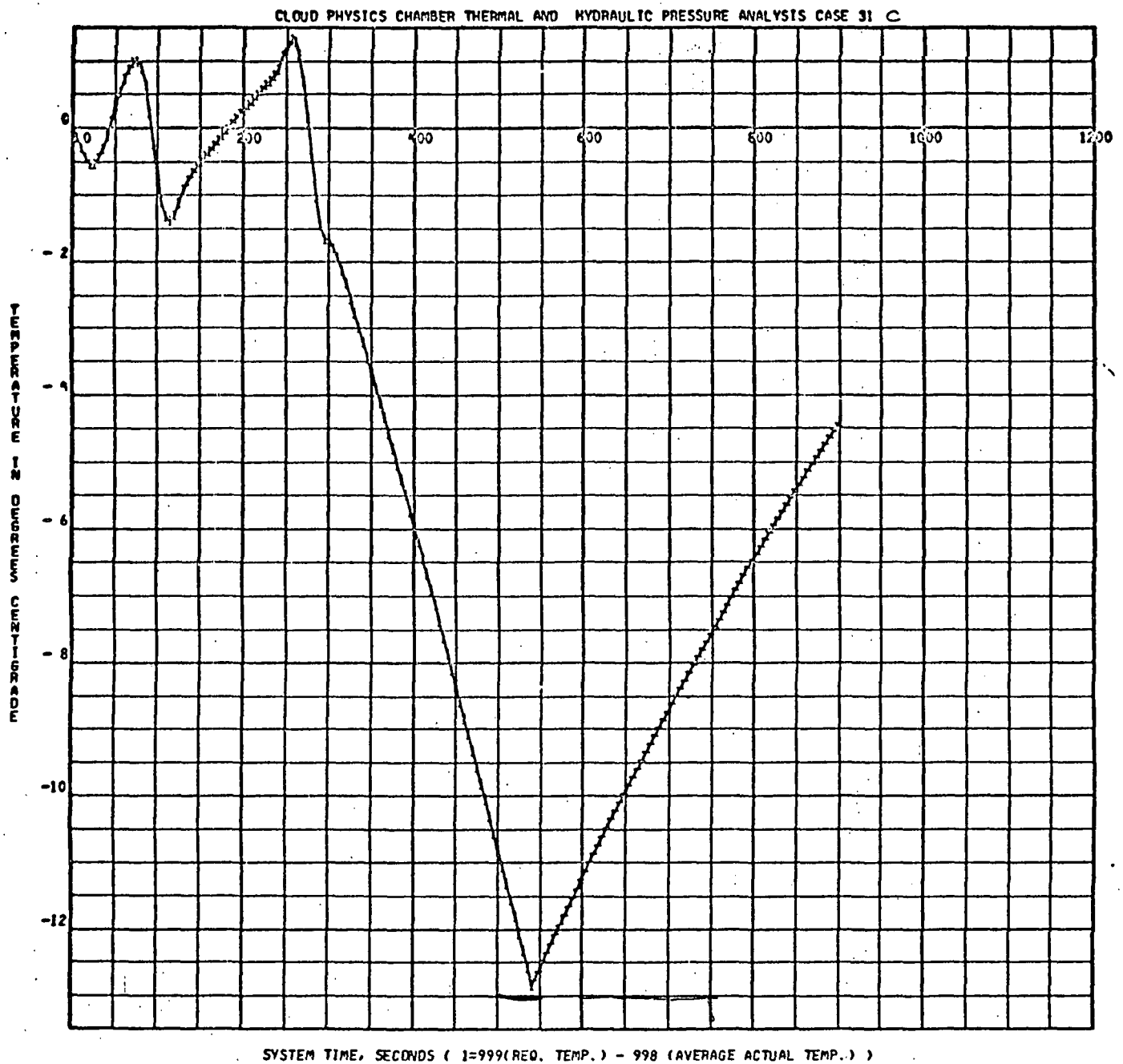

Figure 10. Configuration "4" Deviation from Required Temperature Case 31c.

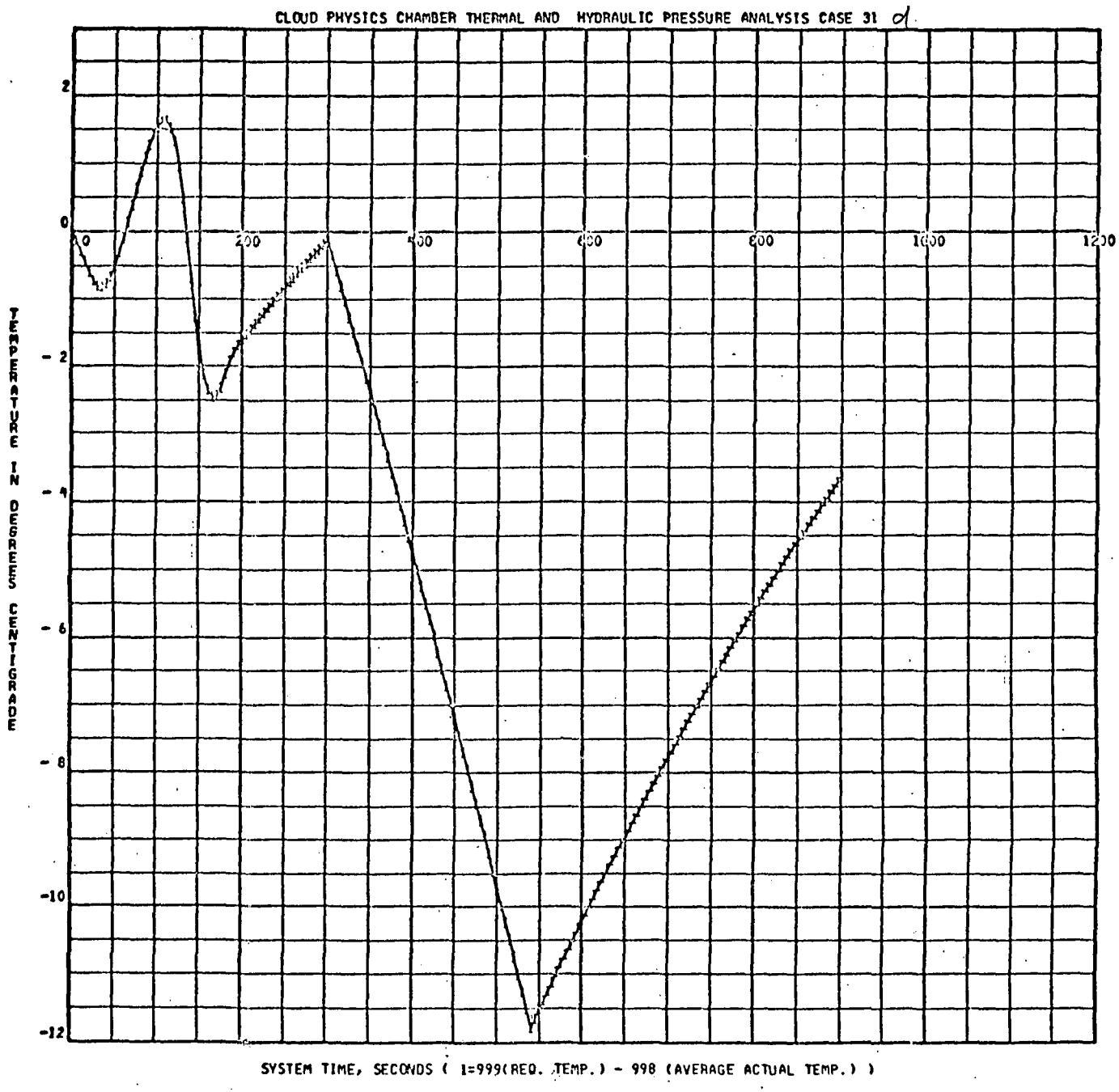

Figure 11. Configuration "4" Deviation from Required Temperature Case 31d.

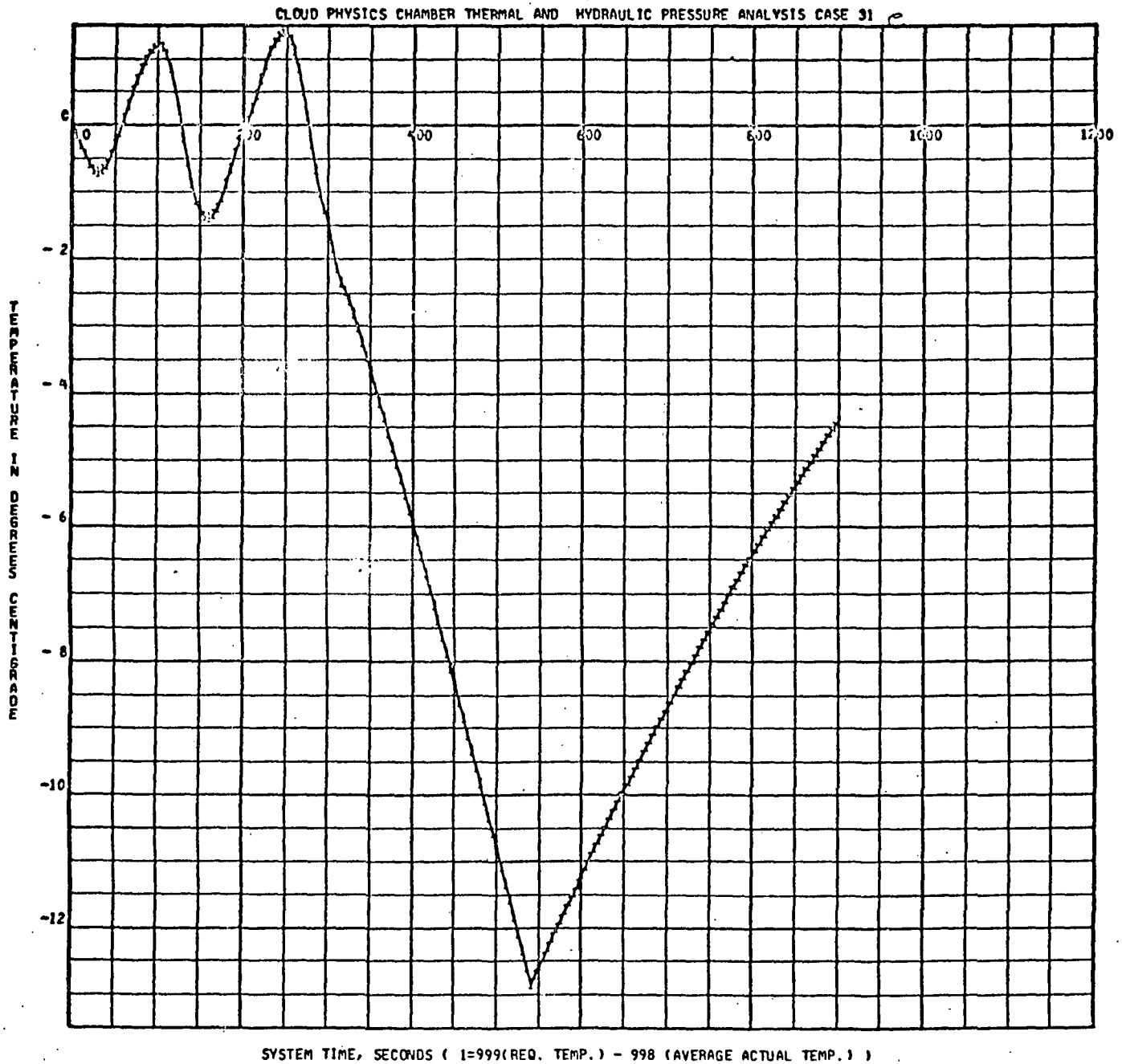

Figure 12. Configuration "4" Deviation from Required Temperature Case 31e.

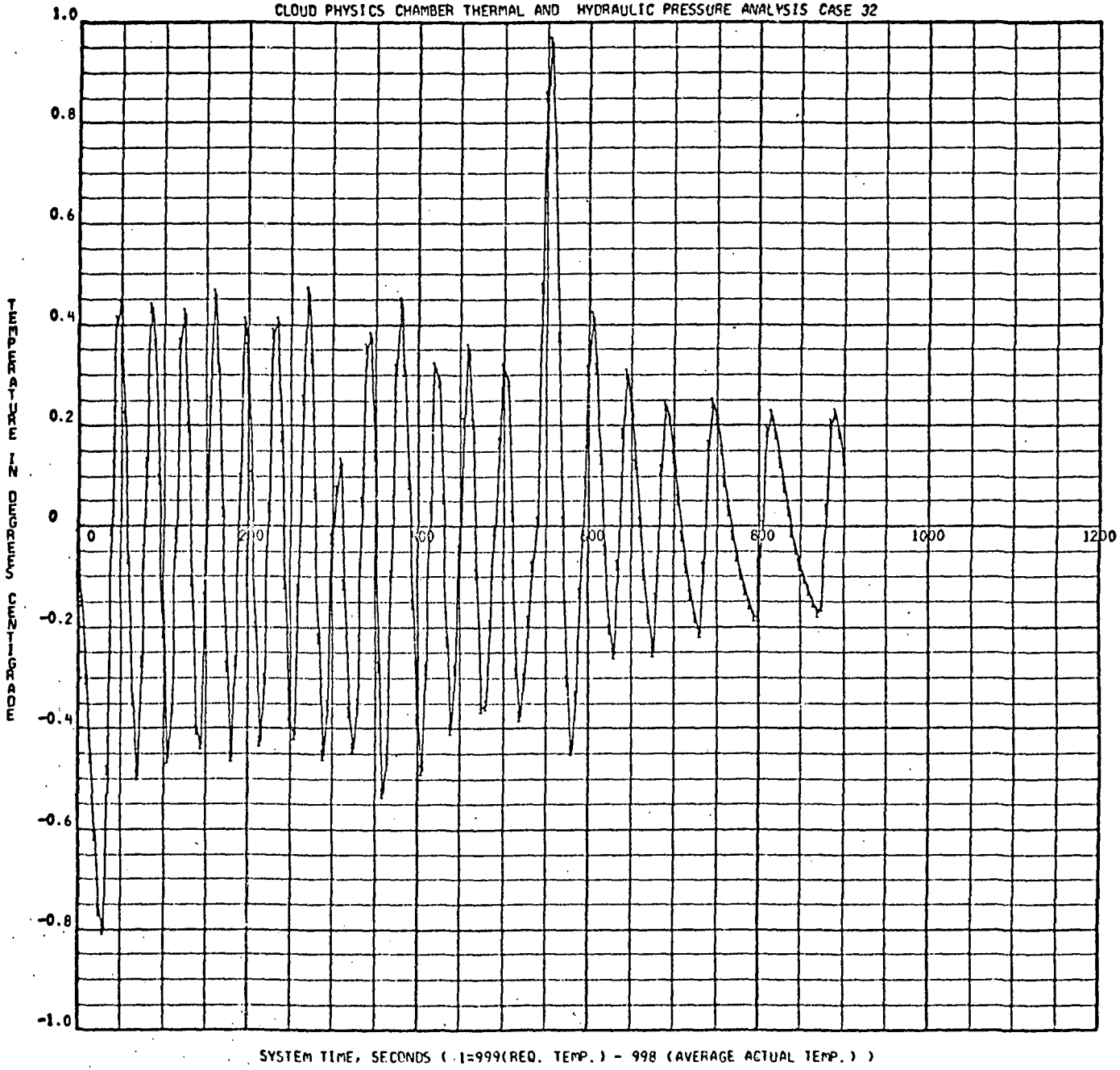

Figure 13. Configuration "4" Deviation from Required Temperature Case 32a.

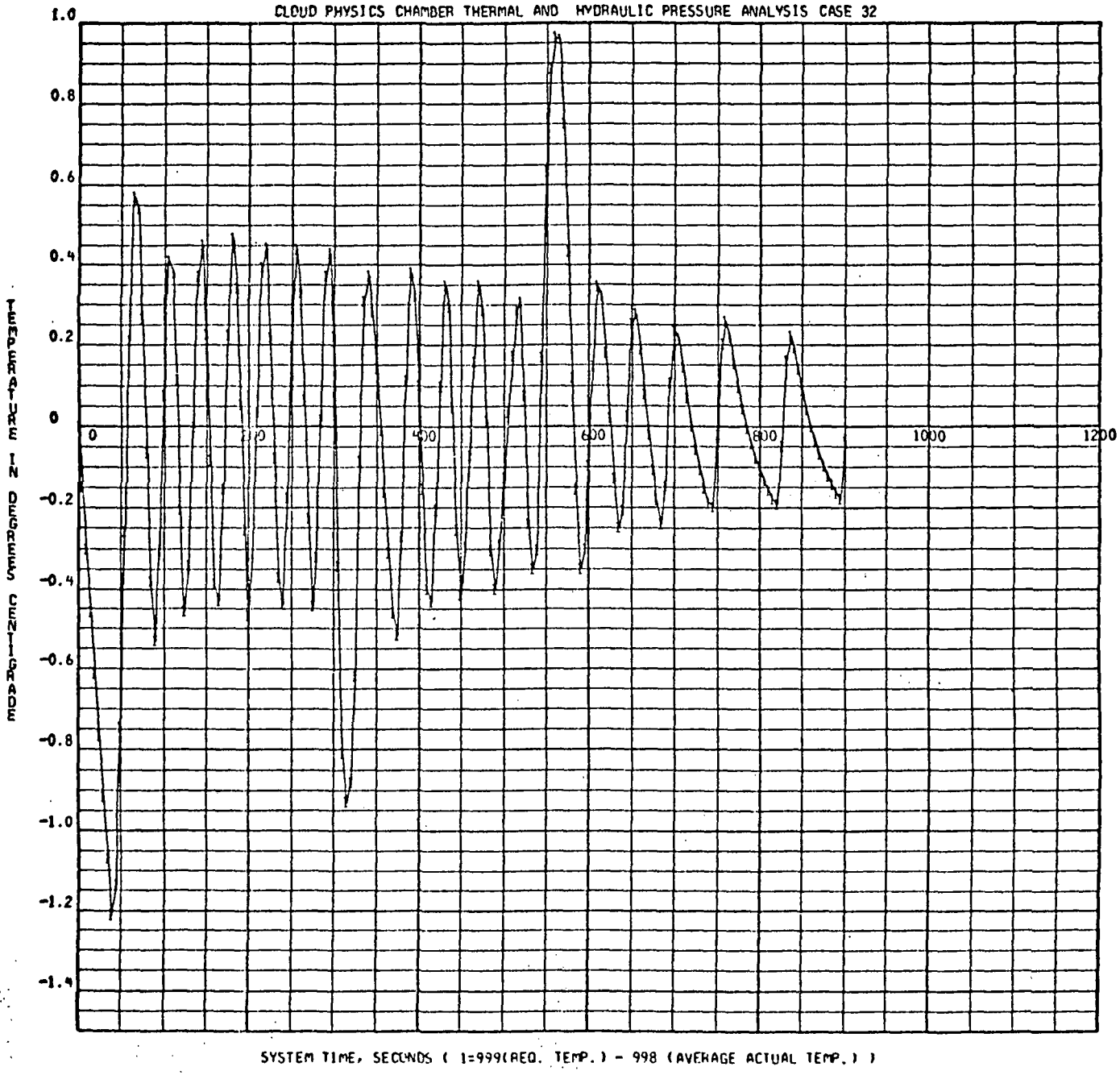

Figure 14. Configuration "4" Deviation from Required Temperature Case 32b.

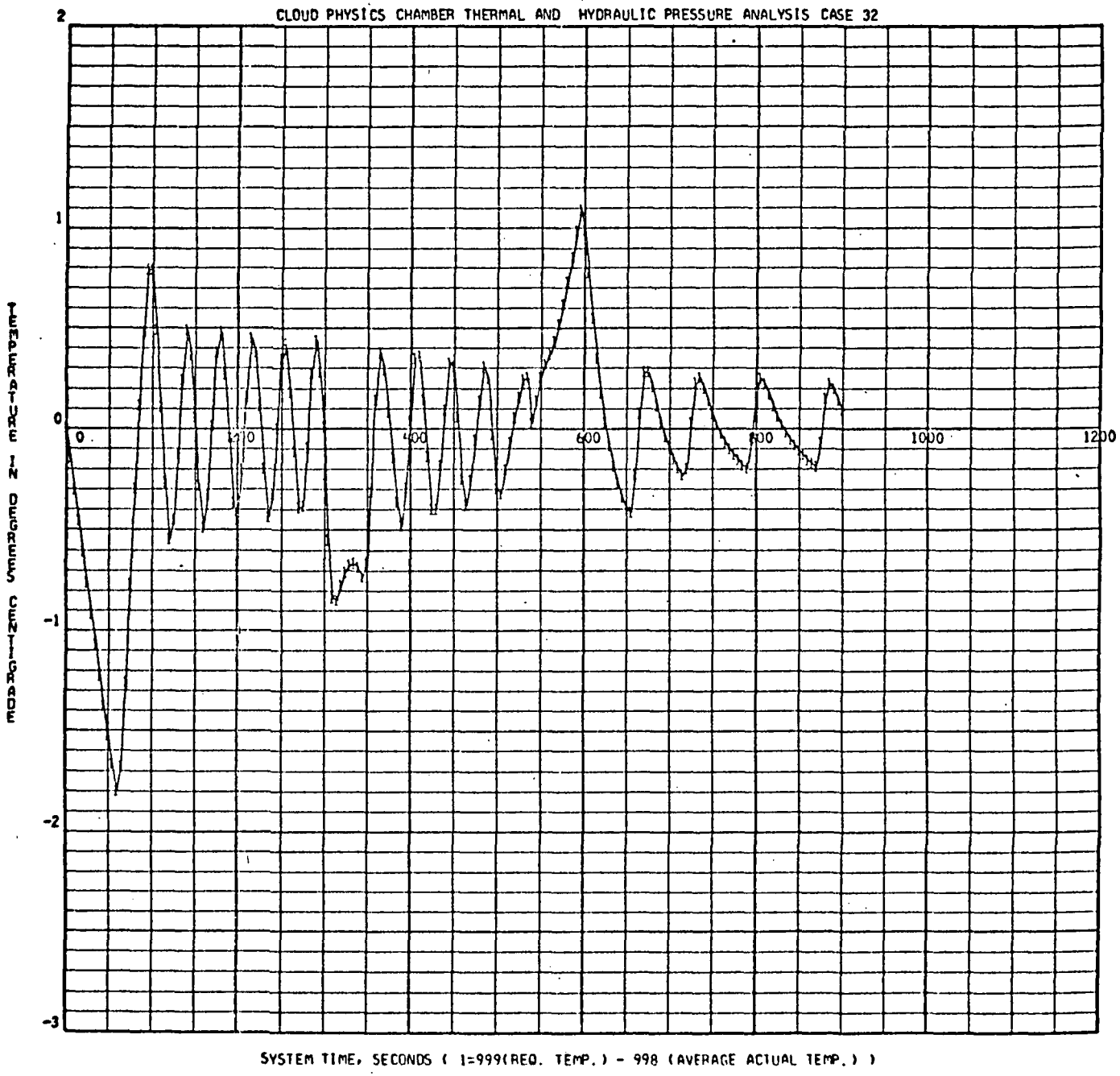

Figure 15. Configuration "4" Deviation from Required Temperature Case 32c.

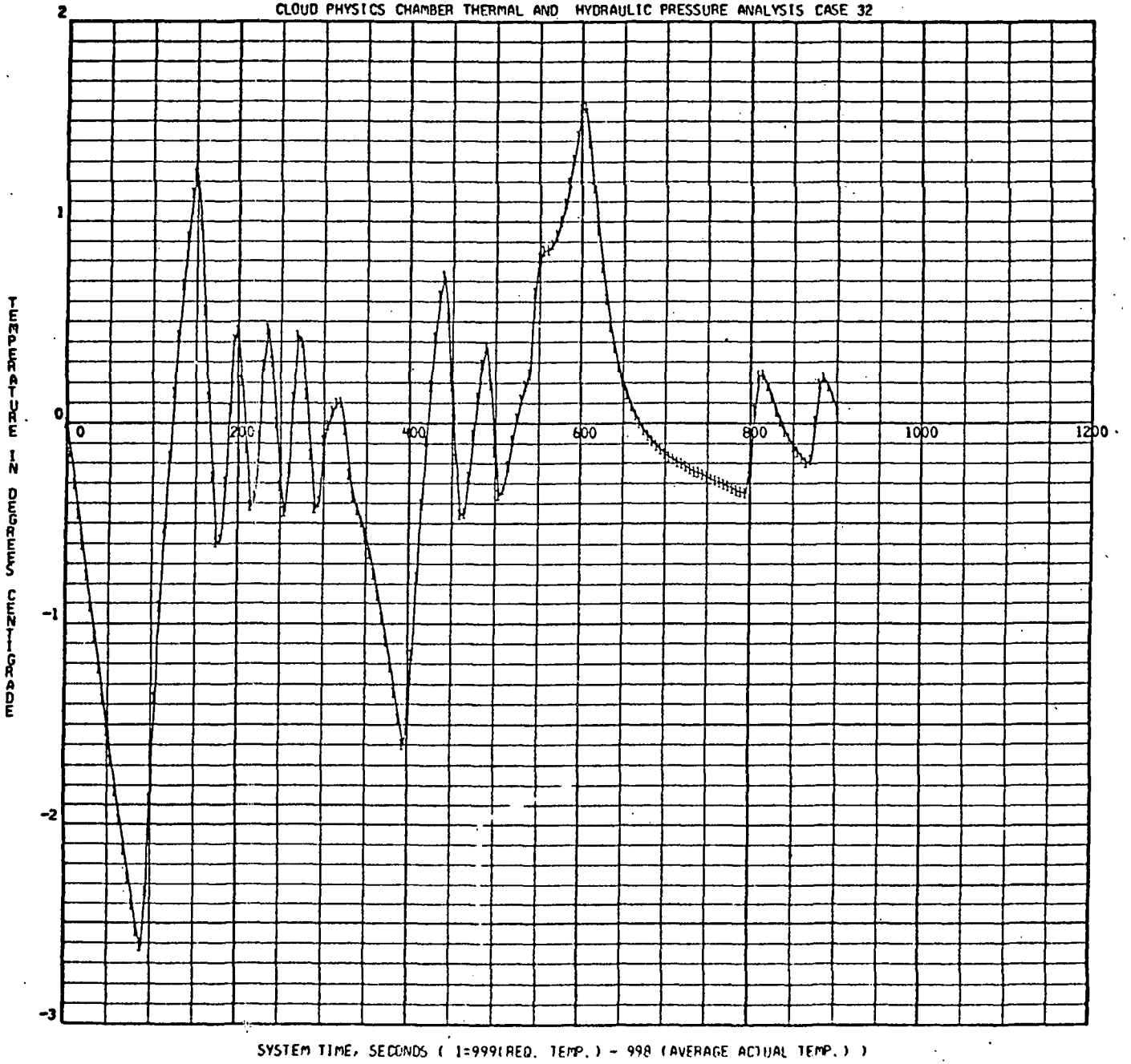

Figure 16. Configuration "4" Deviation from Required Temperature Case 32d.

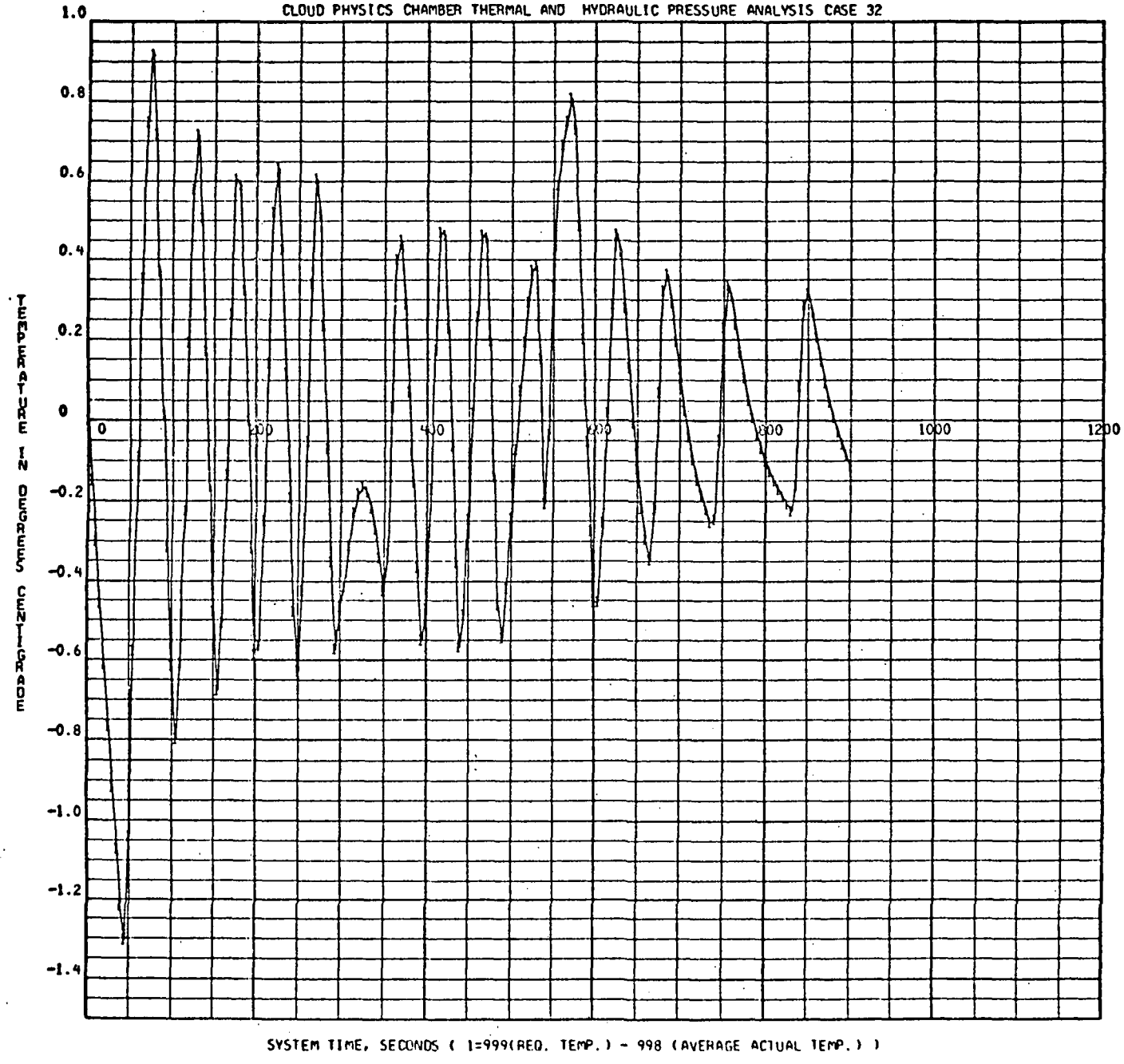

Figure 17. Configuration "4" Deviation from Required Temperature Case 32e.

Figure 18. Configuration "4" Deviation from Required Temperature Case 32f.

THIS PLOT WAS NOT RECEIVED.

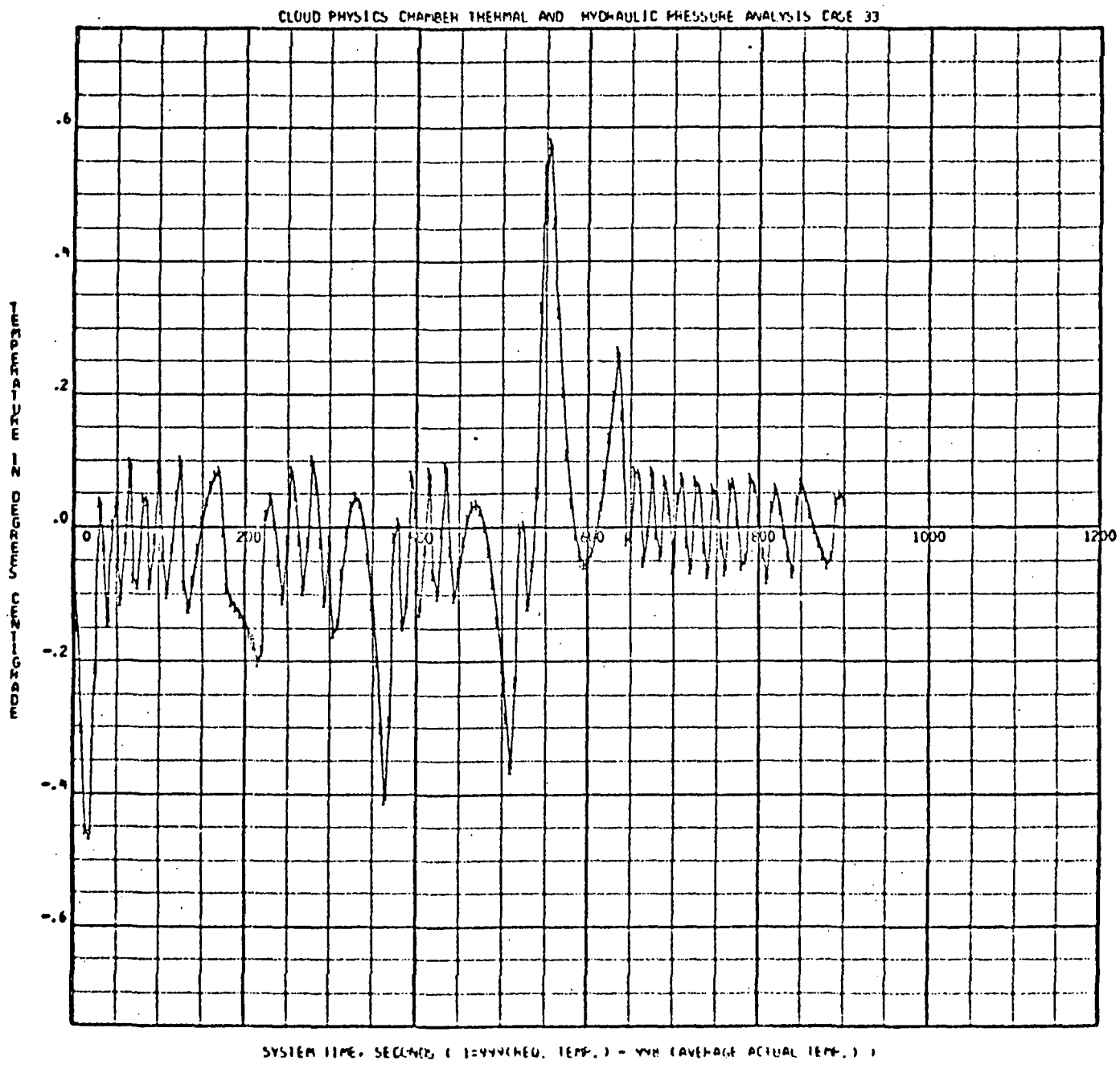

Figure 19. Configuration "5" Deviation from Required Temperature Case 33a.

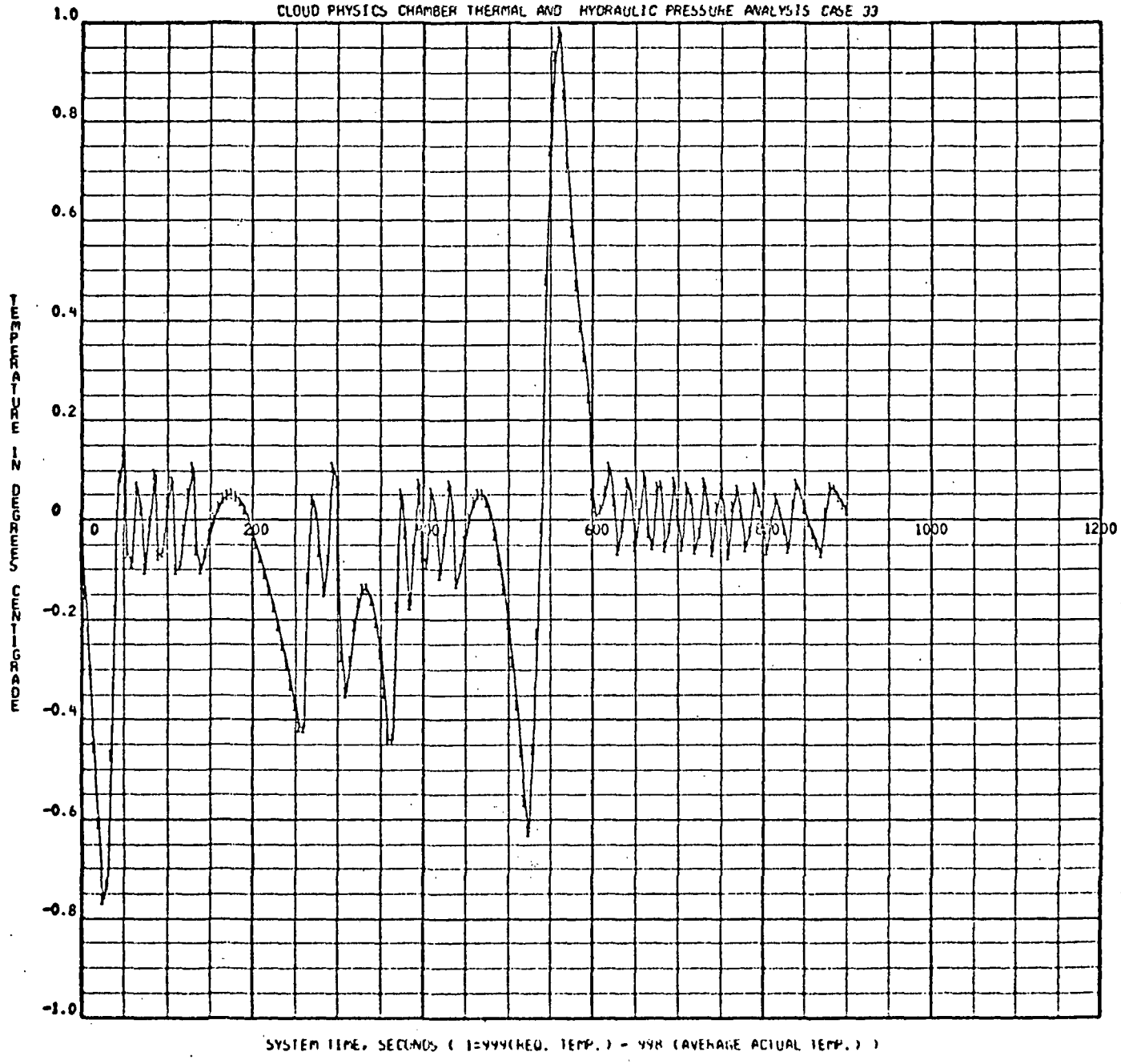

Figure 20. Configuration "5" Deviation from Required Temperature Case 33b.

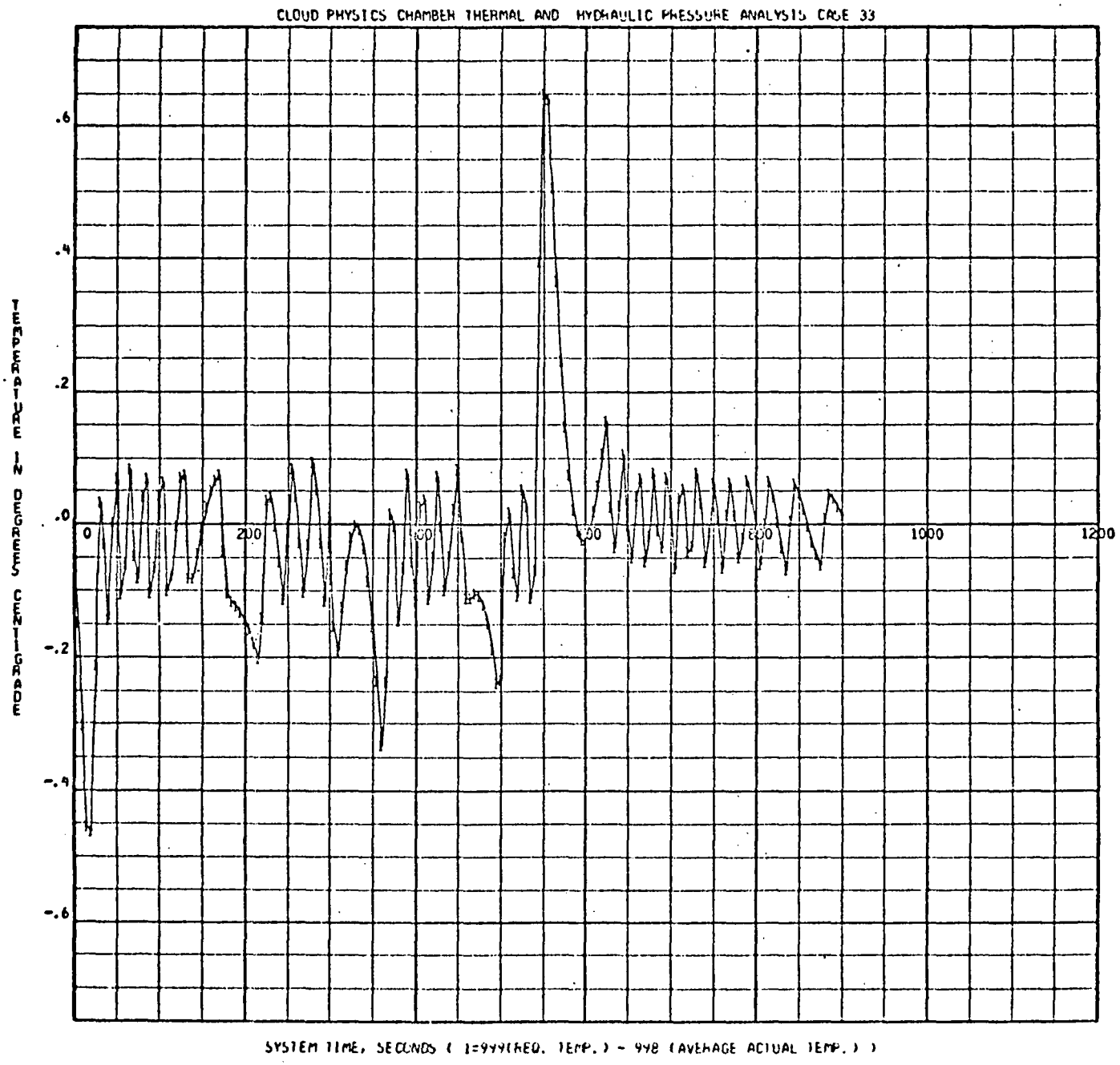

Figure 21. Configuration "5" Deviation from Required Temperature Case 33c.

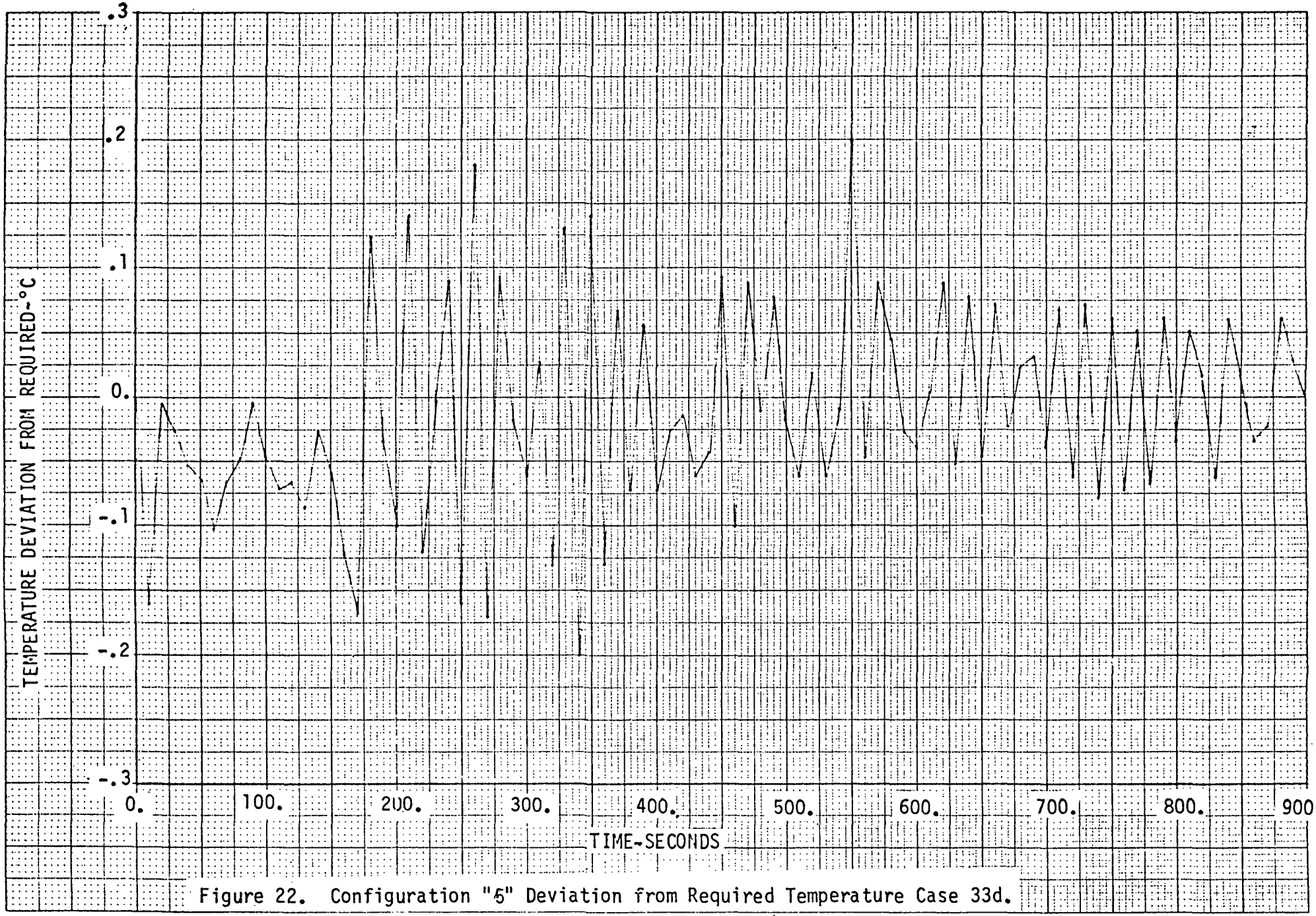

Figure 22. Configuration "5" Deviation from Required Temperature Case 33d.

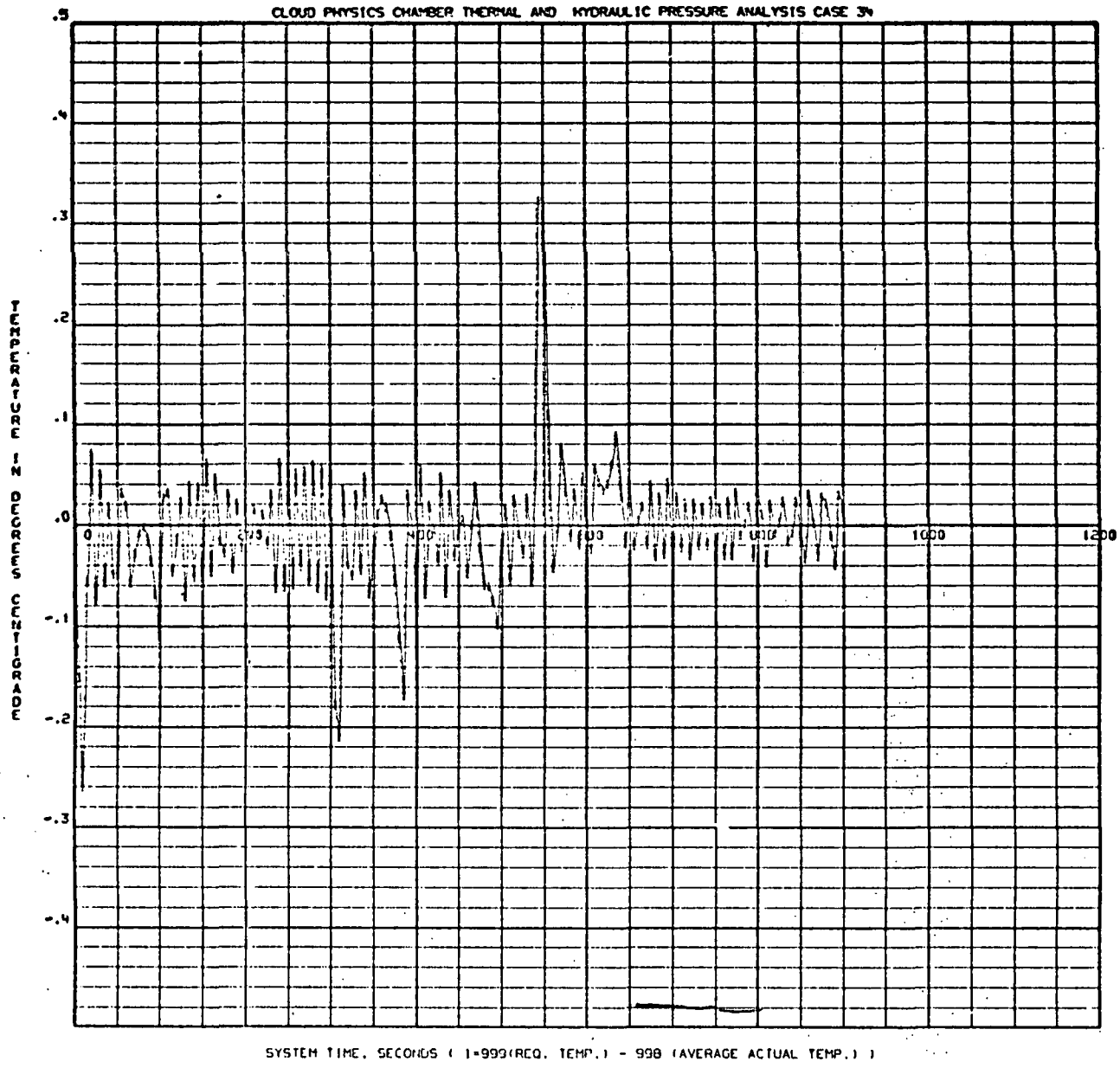

Figure 23. Configuration "5" Deviation from Required Temperature Case 34a.

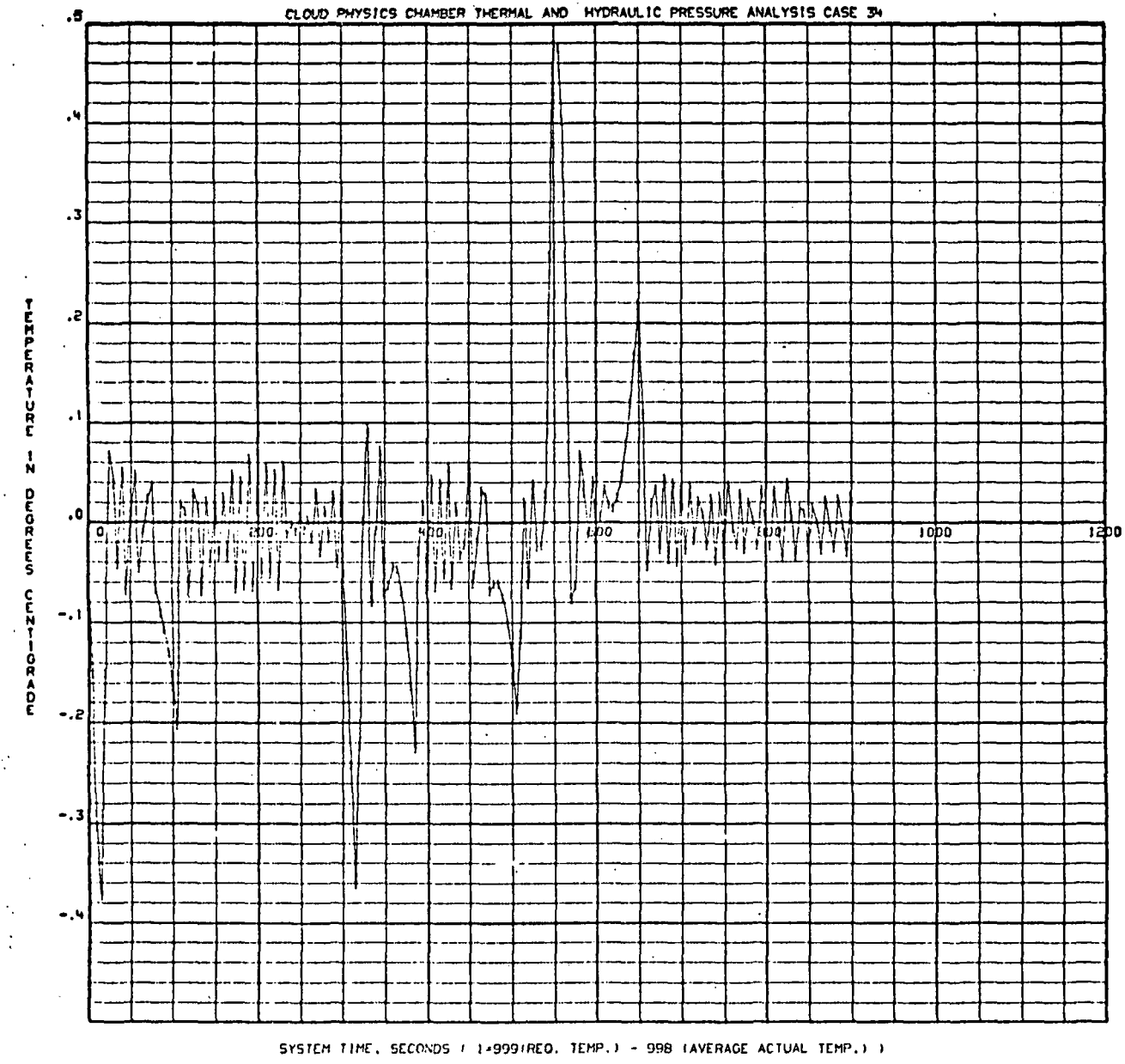

Figure 24. Configuration "5" Deviation from Required Temperature Case 34b.

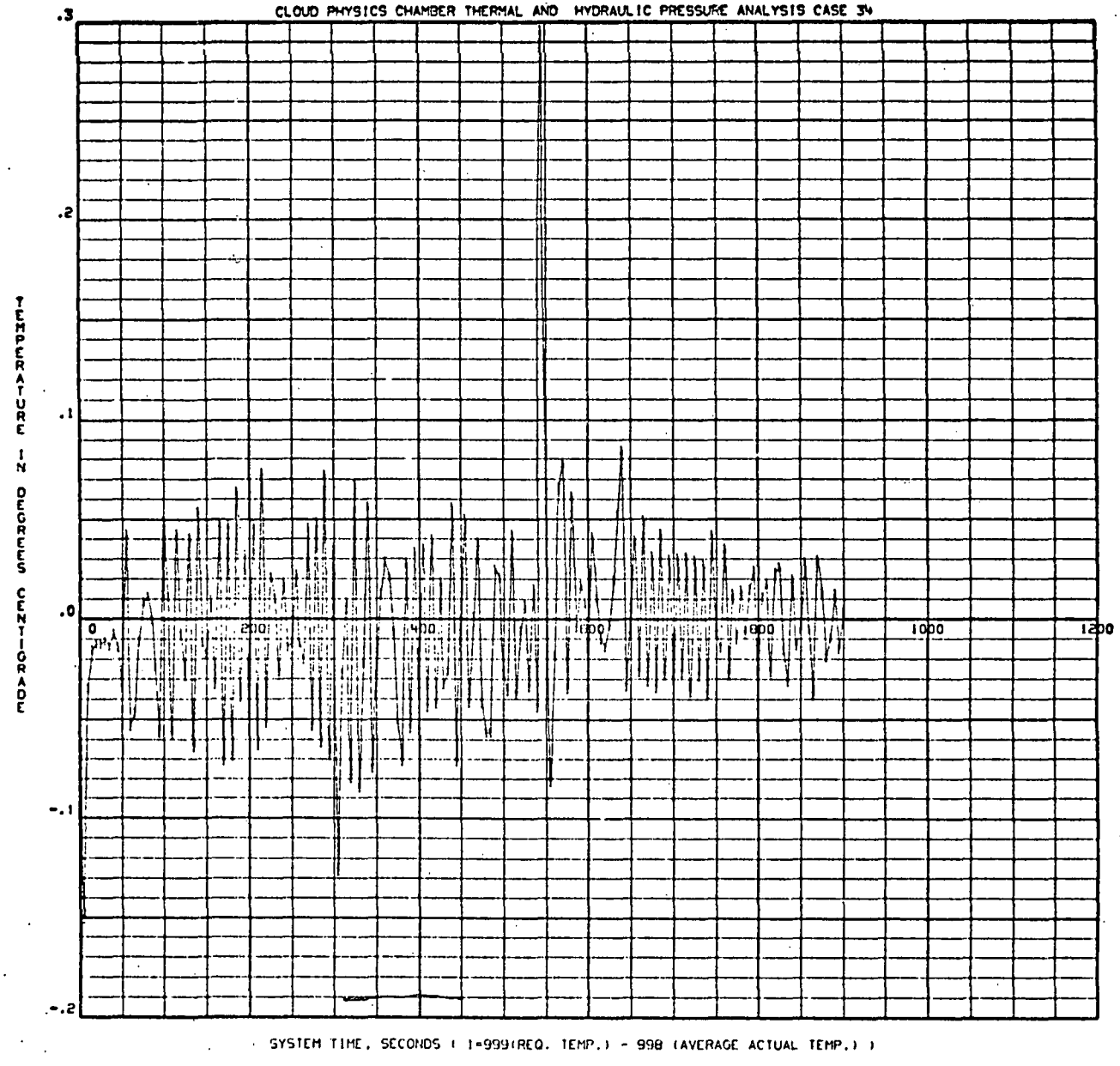

Figure 25. Configuration "5" Deviation from Required Temperature Case 34c.

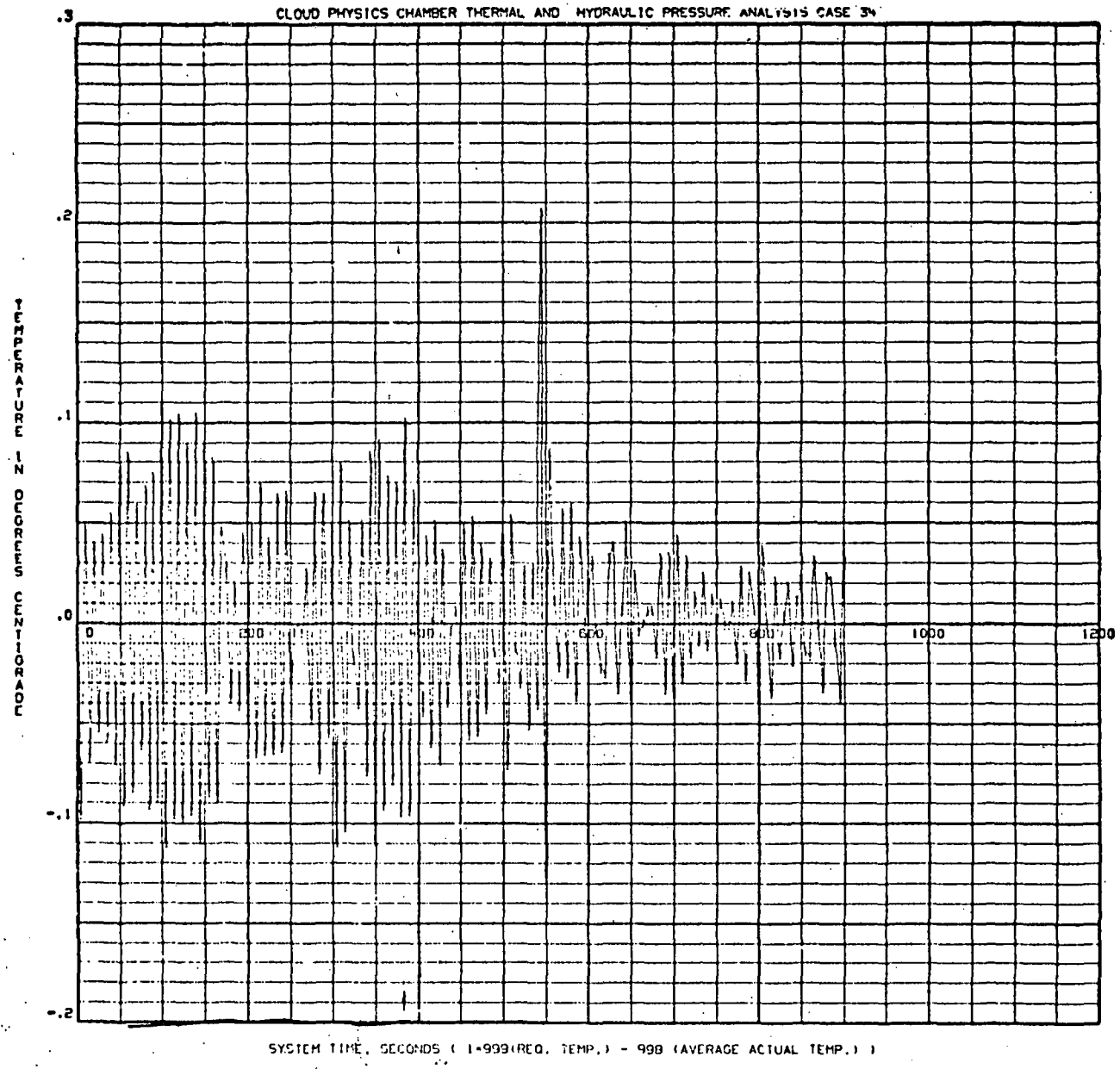

Figure 26. Configuration "5" Deviation from Required Temperature Case 34d.

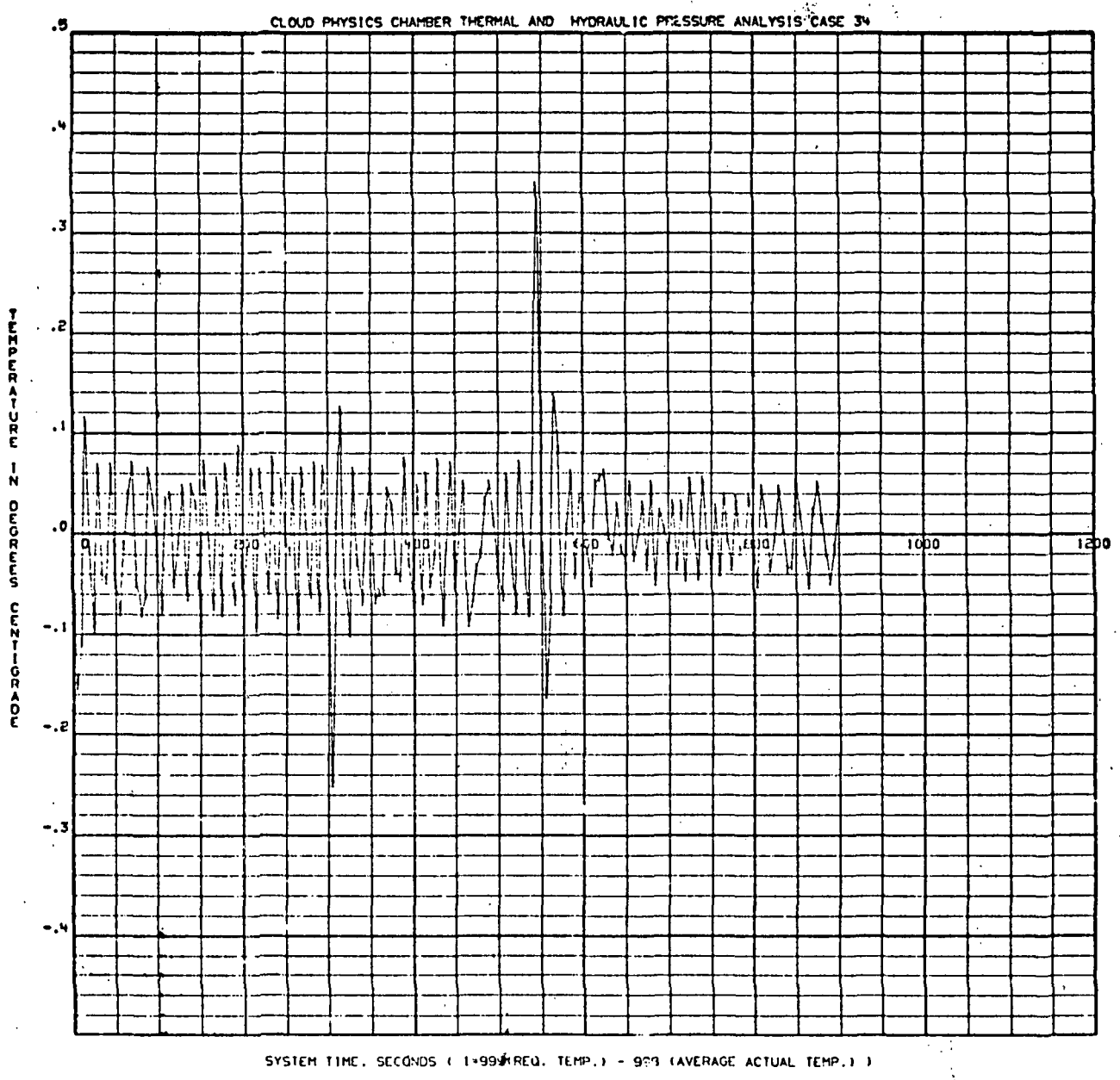

Figure 27. Configuration "5" Dev iation from Required Temperature Case 34e.

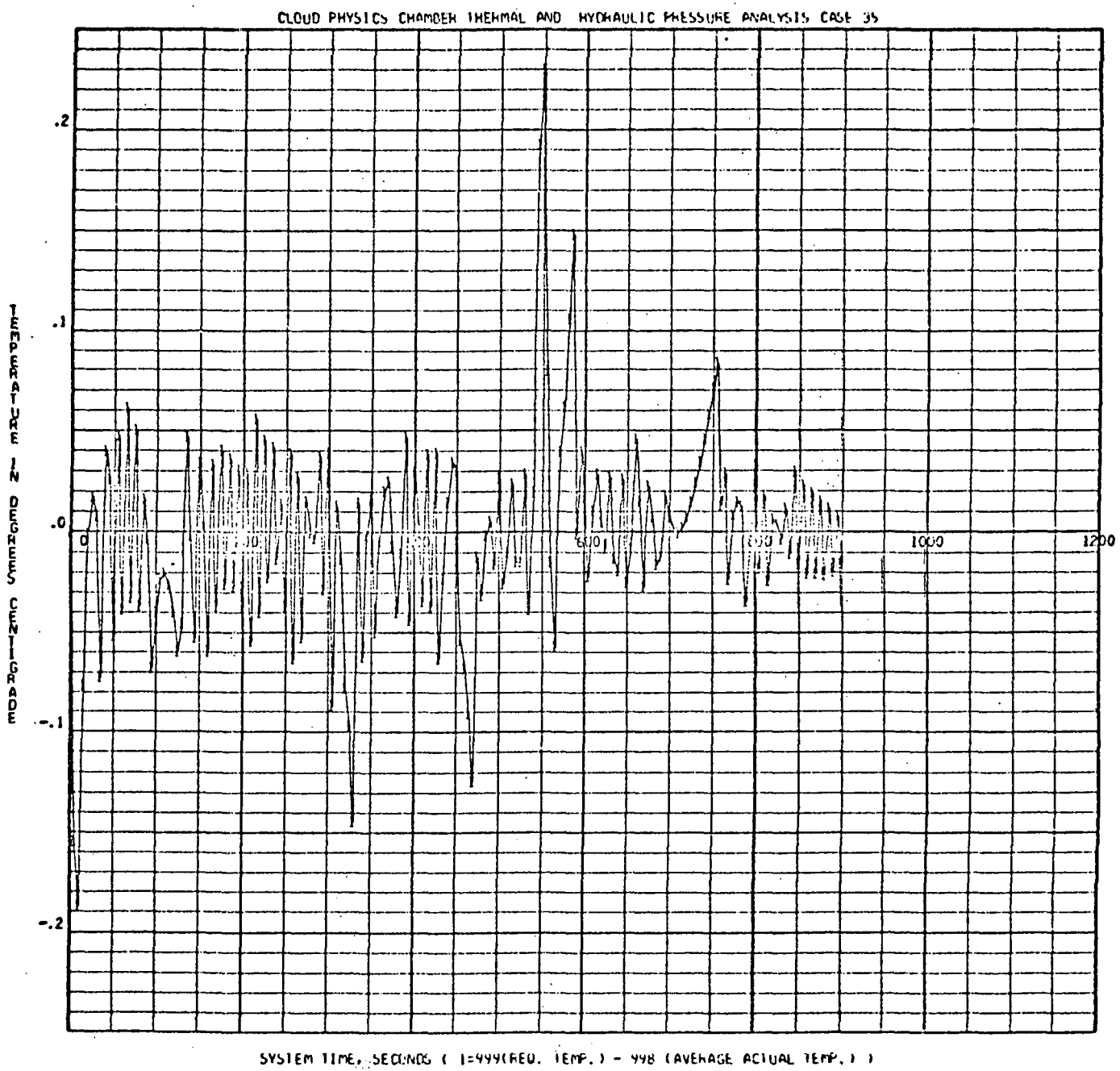

Figure 28. Configuration "5" Deviation from Required Temperature Case 35a.

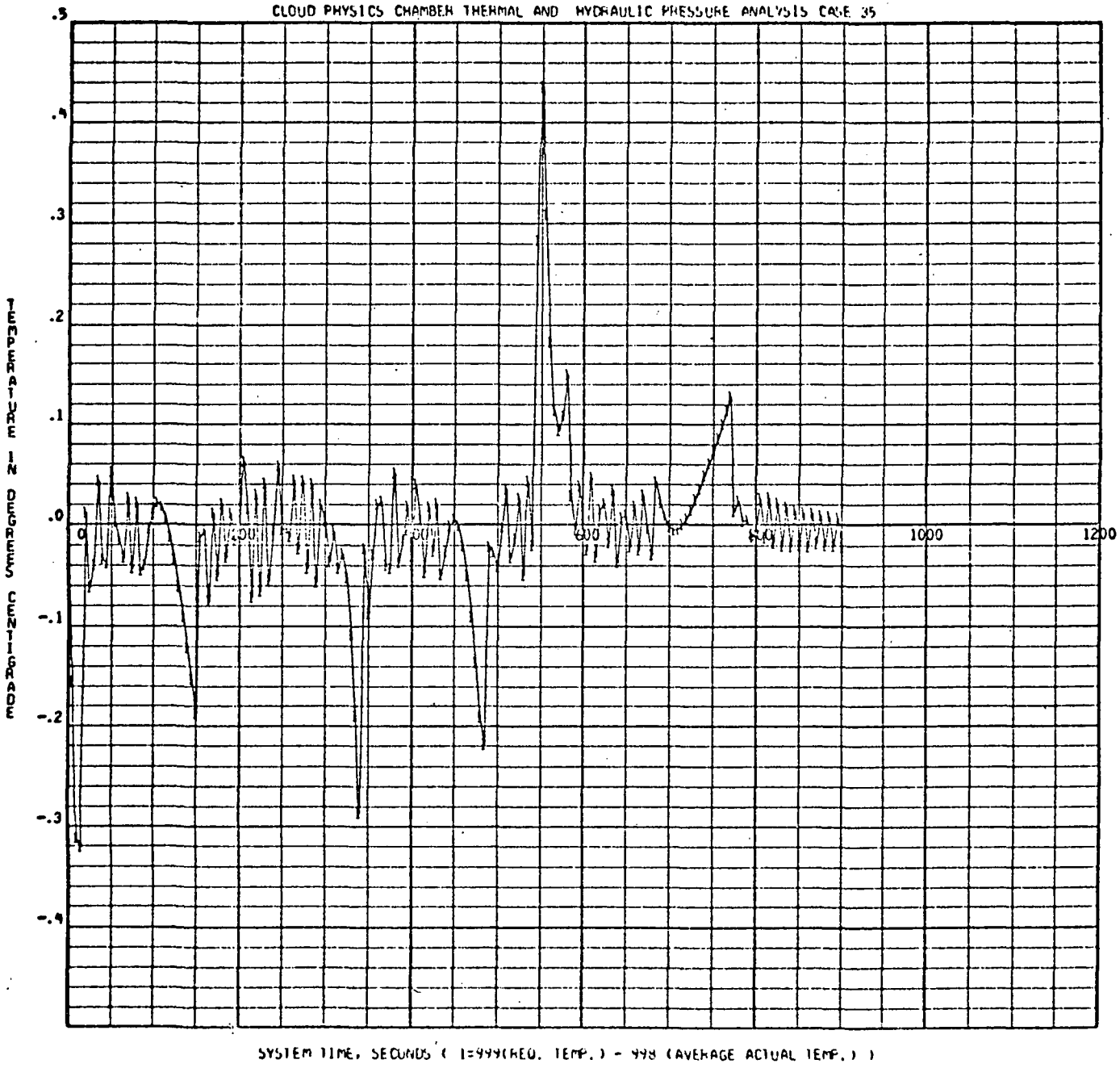

Figure 29. Configuration "5" Deviation from Required Temperature Case 35b.

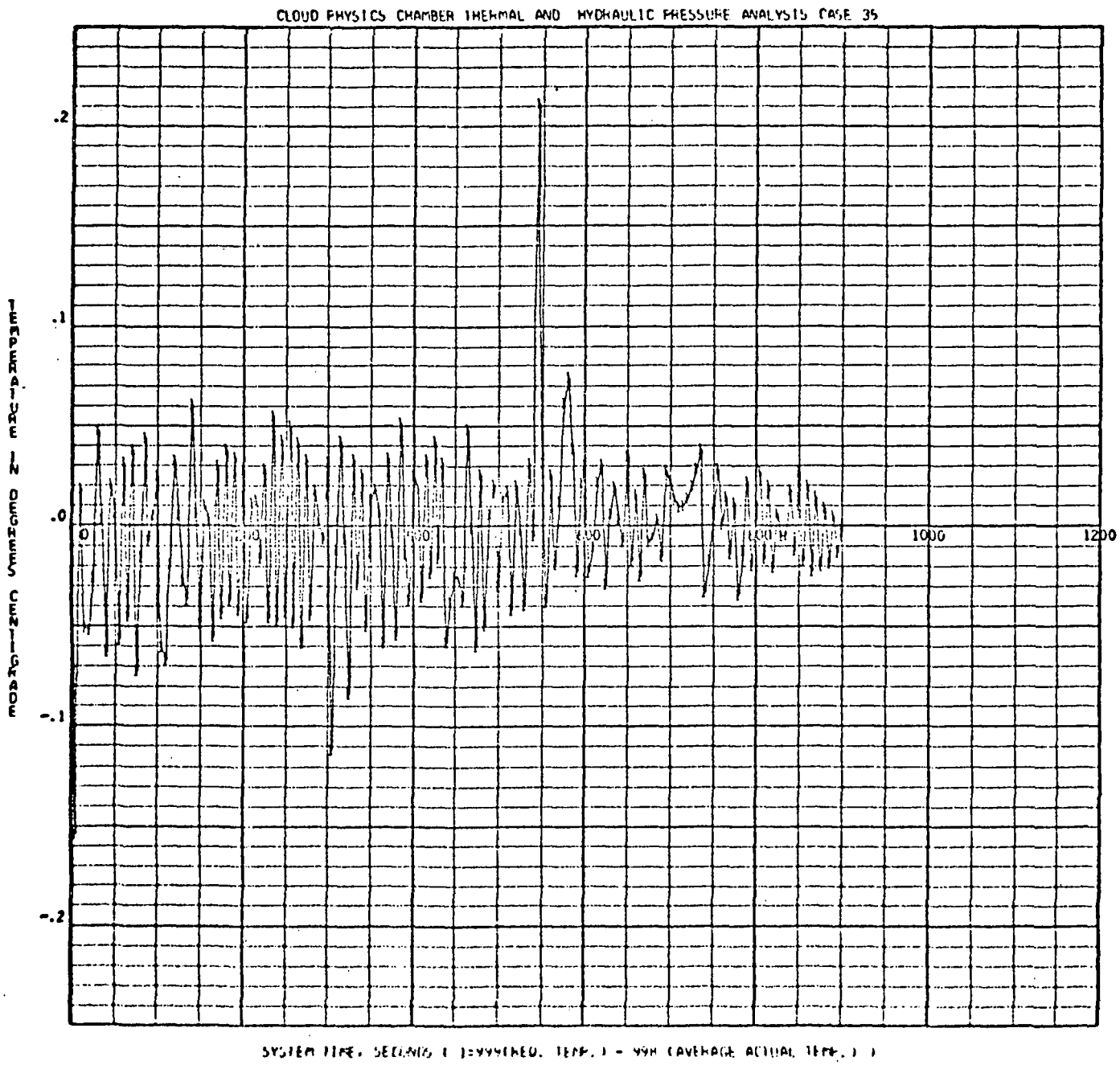

Figure 30. Configuration "5" Deviation from Required Temperature Case 35c.

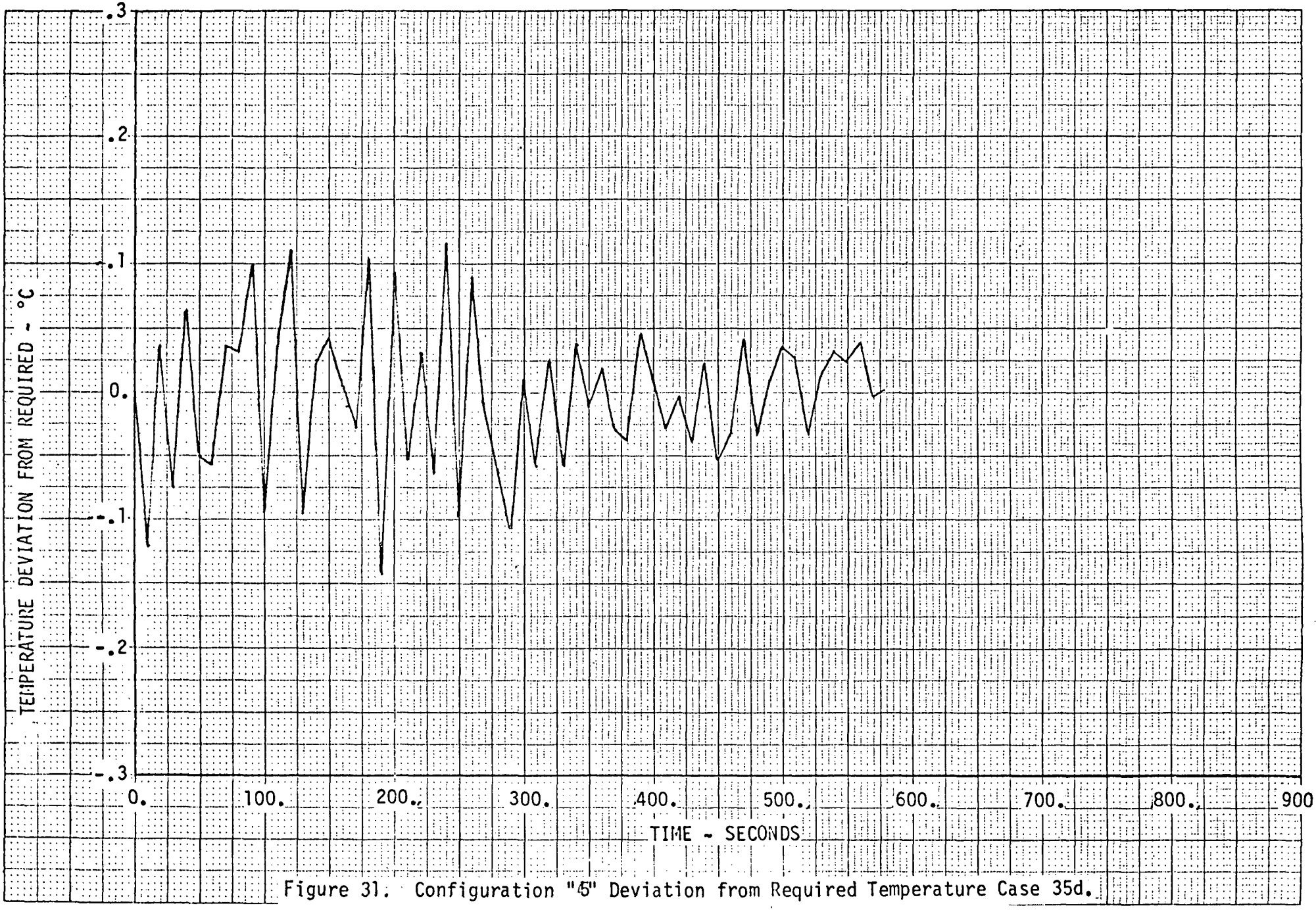

Figure 31. Configuration "5" Deviation from Required Temperature Case 35d.

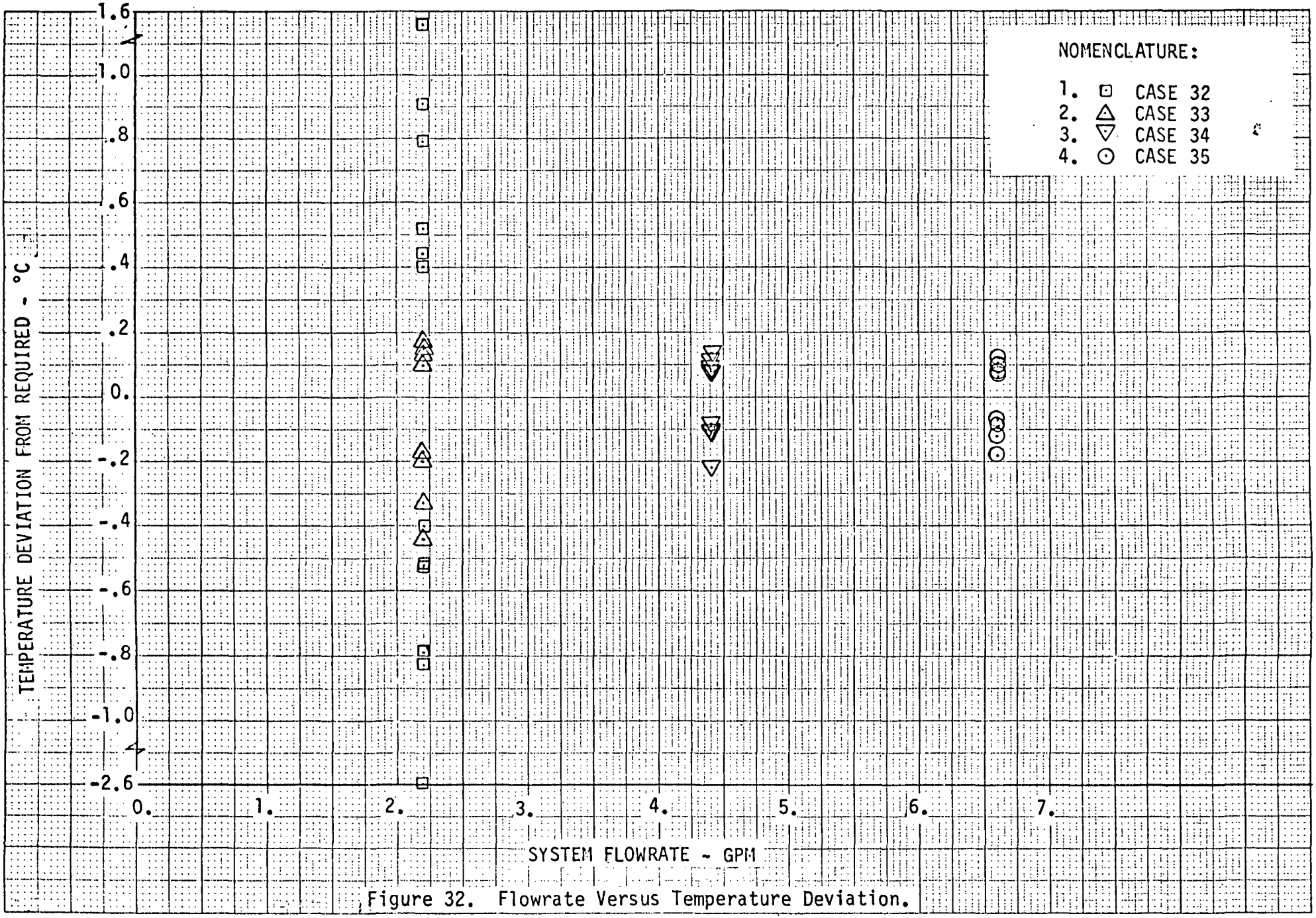

Figure 32. Flowrate Versus Temperature Deviation.

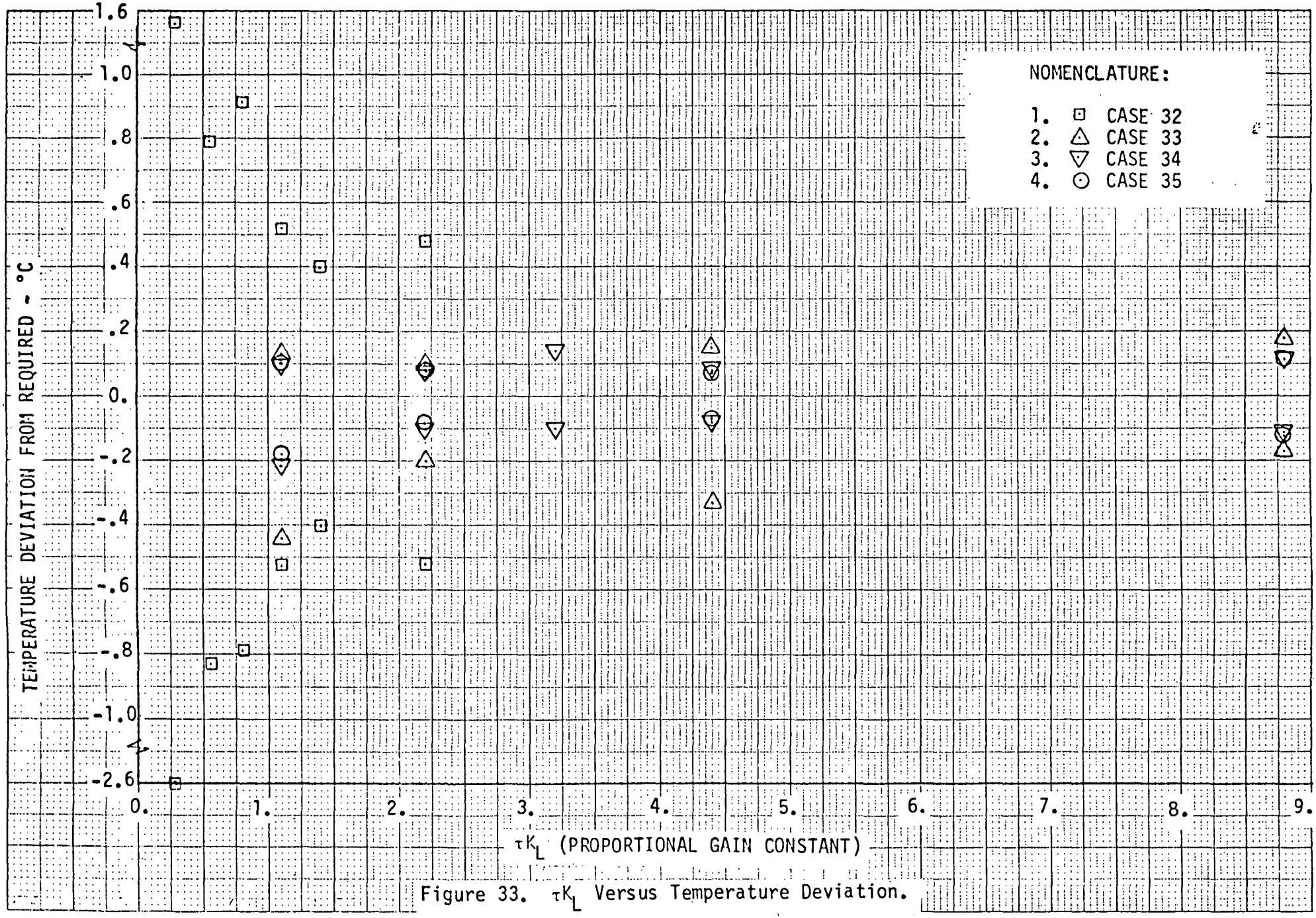

Figure 33. τK_L Versus Temperature Deviation.